2022-03

Non-invasive transcranial ultrasound stimulation for neuromodulation

Darmani, G

10.1016/j.clinph.2021.12.010
Clinical Neurophysiology
Elsevier BV

Non-invasive transcranial ultrasound stimulation for neuromodulation

G. Darmani[1*], T.O. Bergmann[2,3], K. Butts Pauly[4,5,6], C. F. Caskey [7,8], L. de Lecea[9], A. Fomenko[1], E. Fouragnan[10], W. Legon[11], K.R. Murphy[9], T. Nandi [2], M.A. Phipps[7,8], G. Pinton[12], H. Ramezanpour[13], J. Sallet[14,15], S.N. Yaakub[10], S.S. Yoo[16], R. Chen[1,17*]

[1] Krembil Research Institute, University Health Network, Toronto, Canada

[2] Neuroimaging Center (NIC), Focus Program Translational Neuroscience (FTN), Johannes Gutenberg University Medical Center, Mainz, Germany

[3] Leibniz Institute for Resilience Research, Mainz, Germany

[4] Department of Bioengineering, Stanford University, Stanford, CA, USA

[5] Department of Electrical Engineering, Stanford University, Stanford, CA, USA

[6] Department of Radiology, Stanford University, Stanford, CA, USA

[7] Vanderbilt University Institute of Imaging Science, Vanderbilt University, Nashville, TN, USA

[8] Department of Radiology and Radiological Sciences, Vanderbilt University Medical Center, Nashville, TN, USA

[9] Department of Psychiatry and Behavioral Sciences, Stanford University, Stanford, CA, USA

[10] School of Psychology, University of Plymouth, Plymouth, UK

[11] Department of Neurological Surgery, School of Medicine, University of Virginia, Charlottesville, VA, USA

[12] Joint Department of Biomedical Engineering, University of North Carolina at Chapel Hill and the North Carolina State University, Chapel Hill, NC, USA

[13] Centre for Vision Research, York University, Toronto, Ontario, Canada

[14] Univ Lyon, Université Lyon 1, Inserm, Stem Cell and Brain Research Institute, Bron, France

[15] Wellcome Centre for Integrative Neuroimaging, Department of Experimental Psychology, University of Oxford, Oxford, United Kingdom

[16] Department of Radiology, Brigham and Women's Hospital, Harvard Medical School, Boston, MA, USA

[17] Division of Neurology, Department of Medicine, University of Toronto, Toronto, Canada

* Correspondence should be addressed to: Ghazaleh Darmani (ghazaleh.darmani@uhnresearch.ca) or Robert Chen (robert.chen@uhn.ca).

Highlights

- Transcranial ultrasound stimulation (TUS) has higher spatial resolution and deeper penetration compared to other non-invasive stimulation methods.
- TUS can produce short-term and long-lasting changes in neuronal excitability and spontaneous firing rate of neurons.
- TUS holds great potential as an investigative tool in neuroscience and as a treatment for neurological and psychiatric disorders.

Abstract

Transcranial ultrasound stimulation (TUS) holds great potential as a tool to alter neural circuits non-invasively in both animals and humans. In contrast to established non-invasive brain stimulation methods, ultrasonic waves can be focused on both cortical and deep brain targets with the unprecedented spatial resolution as small as a few cubic millimeters. This focusing allows exclusive targeting of small subcortical structures, previously accessible only by invasive deep brain stimulation devices. The neuromodulatory effects of TUS are likely derived from the kinetic interaction of the ultrasound waves with neuronal membranes and their constitutive mechanosensitive ion channels, to produce short term and long-lasting changes in neuronal excitability and spontaneous firing rate. After decades of mechanistic and safety investigation, the technique has finally come of age, and an increasing number of human TUS studies are expected. Given its excellent compatibility with non-invasive brain mapping techniques, such as electroencephalography (EEG) and functional magnetic resonance imaging (fMRI), as well as neuromodulatory techniques, such as transcranial magnetic stimulation (TMS), systemic TUS effects can readily be assessed in both basic and clinical research. In this review, we present the fundamentals of TUS for a broader audience. We provide up-to-date information on the physical and neurophysiological mechanisms of TUS, available readouts for its neural and behavioral effects, insights gained from animal models and human studies, potential clinical applications, and safety considerations. Moreover, we discuss the indirect effects of TUS on the nervous system through peripheral co-stimulation and how these confounding factors can be mitigated by proper control conditions.

Keywords: Transcranial ultrasound stimulation, neuromodulation, plasticity, non-invasive brain stimulation

1. Introduction

The use of ultrasound for neuromodulation has a long history dating back to the 1920's when E. Newton Harvey explored the effect of sound waves on biological tissues. He classified "stimulation of cells" as one of its biological effects and, in 1929, described its effect on neuronal tissue (Harvey, 1929). In the 1950s, the Fry brothers reported reversible suppression of spontaneous neuronal spiking upon ultrasound exposure (Fry et al., 1951) and, in 1958, William Fry targeted the lateral geniculate nucleus of cats using focused ultrasound to suppress visual-evoked potentials recorded in the visual cortex (Fry et al., 1958). Despite decades of evidence demonstrating the effects of ultrasound on the nervous system (Takagi et al., 1960; Lele, 1963; Gavrilov et al., 1996; Velling and Shklyaruk, 1998), ultrasound went largely unrecognized as an effective non-invasive form of neuromodulation. In the late 2000's, ultrasound neuromodulation went through a renaissance period with the findings of William Tyler who showed ultrasound opened voltage gated Na^+ and Ca^{2+} channels in hippocampal slice cultures (Tyler et al., 2008). In 2010, his group showed that ultrasound produced motor responses in awake mice when focused on the motor cortex (Tufail et al., 2010). Since these seminal findings, there has been renewed interest in the use of ultrasound for transient brain modulation with numerous discoveries in animal models and human subjects.

2. Physics of Ultrasound

Sound is a pressure, or mechanical, wave that is produced when an object oscillates at a given fundamental frequency (f_0). "Ultrasound" specifically refers to sound waves with frequency above the range of human hearing (f_0 > 20 kHz). To generate ultrasound waves, a material which expands or contracts with applied voltage creates propagating pressure wave fronts at a rate determined by voltage polarity reversal; these materials are commonly referred to as transducers. At low amplitude, the pressure wave propagates as a sinusoidal waveform (Figure 1) with a wavelength (λ) and a fundamental frequency. The period (T) is the time for one cycle ($T=1/f_0$). As an example, at 500 kHz the period is 2 μs, meaning it would take ultrasound 2 μs to travel the length of one wave (λ). The speed of sound (c) is about 1500 m/s in soft tissue and approximately double that in bone. The speed of sound in any given medium is inversely related to its compressibility. Since bone is resistant to compression, sound is transmitted through it relatively quickly. The fundamental frequency, the wavelength, and the speed of sound are related by the equation $c = f_0\lambda$. This equation is useful for calculating the wavelength in different tissues. For example, the wavelength of a f_0=500 kHz wave is approximately 3 mm in soft tissue and 6 mm in bone. In diagnostic ultrasound imaging, the resolution is inversely related to λ, and frequencies from 1-10 MHz are used to obtain good resolution. On the other hand, in ultrasound neuromodulation, there are multiple considerations in the choice of fundamental frequency (cf. section 9.3).

Figure 2A provides some temporal characteristics of ultrasound. The amplitude of the pressure wave is given in pascals (Pa). Another useful measure of the amplitude is the intensity, where the intensity at one point in time is related to the pressure at that same point by $I = \frac{P^2}{Z}$, where Z is the acoustic impedance ($Z = \rho c$, in which ρ is the density of the medium). The units for intensity are $(\frac{W}{cm^2})$, which is the power per unit area. The time average intensity of the sinusoidal pressure wave is related to the peak pressure by $I = \frac{P_{pk}^2}{2Z}$. The spatial peak pulse average intensity (I_{SPPA}) is the time average over a single pulse, while the spatial peak temporal average intensity (I_{SPTA}) is the time average over a train of pulses if the ultrasound is applied in pulsed wave mode (PW). When it is applied as a single continuous pulse in continuous wave mode (CW), then I_{SPTA}=I_{SPPA}.

Figure 2B provides the spatial characteristics of focused ultrasound. A focused transducer is usually used to minimize the focus, while spreading off-target energy across a larger portion of the skull and brain. An example of a simulated focus is shown in Figure 2B, where the beam is coming from the left. The peak pressure or intensity can be measured in a water tank with a hydrophone. This is the ideal focus, and we will discuss how the skull defocuses and diminishes the ultrasound focus.

The spatial and temporal characteristics can be combined, as shown in Figure 2C. The spatial peak pulse average intensity (I_{SPPA}) is the mean over the pulse duration (PD). A pulse is the shortest continuous sonication. The spatial peak temporal average intensity (I_{SPTA}) is the mean over the pulse repetition interval (PRI). For the simple pulsing shown in Figure 2, these are related by $I_{SPTA} = I_{SPPA}DC$. Duty cycle (DC) is defined as the ratio of the time that the ultrasound is on (PD) to the PRI. In the example shown in Figure 2A, a 50% duty cycle is shown. The pulse repetition frequency (PRF) is given by $RF = \frac{1}{PRI}$. In order to reduce the rate of tissue heating in neuromodulation applications for a given peak intensity, ultrasound is often pulsed rather than delivered continuously (Dalecki, 2004; O'Brien, 2007; O'Reilly et al., 2010).

The material properties of tissues highly influence ultrasound propagation. Cerebrospinal fluid, white matter, and gray matter have similar acoustic properties due to their high water content (Mueller et al., 2016). Ultrasound propagates well in aqueous soft tissue and is minimally affected by brain geometry and composition. On the other hand, the properties of bone are quite different from aqueous soft tissues. Bone has high sound speed and attenuation (~20 dB/cm/MHz) compared to the low attenuation in brain tissue (~0.5 dB/cm/MHz). Because attenuation increases with higher frequency, there is an inherent tradeoff with optimal focal size which decreases with higher frequency. Numerical and empirical studies have demonstrated acoustic frequencies < 700 kHz are desired for acceptable loss and focusing through the human skull (Sun and Hynynen, 1998; Clement et al., 2000; Clement and Hynynen, 2002a; White et al., 2006).

Bone thickness can vary from 2-15 mm within and between human skulls, suggesting an 8-fold variation in ultrasound transmission due to thickness alone. However, thickness alone does not account for the variability in ultrasound transmission (Mueller et al., 2017) because the skull is heterogeneous (composed of trabecular and cortical bone) and is shaped differently for different

people. The heterogeneity of bone composition is a critical factor for ultrasound transmission, as scattering dominates attenuation in trabecular bone, while absorption dominates in cortical bone (Bossy et al., 2007; Pinton et al., 2012a). In fact, clinical high intensity focused ultrasound treatments rely on a composition parameter, the skull density ratio (SDR), which is the ratio of the radiodensity in CT Hounsfield units of trabecular to cortical bone (D'Souza et al., 2019; Jung et al., 2019). While this metric does not take into account skull thickness and other sources of intensity loss, it does provide a quick means to evaluate the preponderance of trabecular bone. Local SDR of the area where a low intensity focused ultrasound single element is placed may also prove a useful metric to predict efficacious ultrasound treatment. Lee et al. (2016) had CT scans performed on 19 volunteer participants and found the estimated I_{SPPA} in the brain to vary between individuals from 2.3 to 11.6 W/cm^2 despite delivering the same I_{SPPA} of 16.6 W/cm^2 to the head (Lee et al., 2016b).

3. Acoustic interactions, apertures, and focal spot size

Although a millimetric focus within the brain is feasible with ultrasound, the transducer shape and acoustic interactions have significant impact on the focal spot sizes and locations achievable within the brain. To generate an ultrasound focus through the skull, a transducer is typically coupled to the head via a water or gel path. Sound is emitted from the transducer through the water/gel path and then transmitted through the skull before generating a focus in the brain. When sound is incident on the skull, a significant portion is either reflected or absorbed, and the remainder is transmitted through the skull with altered direction and phase. The degree to which the skull changes the intensity and location of the focus is an aggregate of contributions from multiple acoustic phenomena (Figure 3).

Here, we review common tools used in transcranial ultrasound stimulation (TUS) neuromodulation and highlight the acoustic interactions that are increasingly important for dosimetry and safety as TUS neuromodulation is translated to humans.

A single element transducer shaped like a spherical cap or an array of transducers arranged as a spherical cap focus energy to the center of the sphere from which the cap is cut. The focal spot size generally decreases with increasing aperture size and ultrasound frequency (Figure 4). Because attenuation increases with increasing frequency, researchers typically use low frequencies (<700 kHz) for transcranial ultrasound stimulation. Large hemispherical arrays of approximately 1000 elements have been routinely used for thalamotomy in humans under MR guidance (Clement et al., 2000; Elias et al., 2013). While hemispherical transducers have been successfully used also for neuromodulation (Dallapiazza et al., 2017), whole head shaving and the use of a frame to suspend the head in a water bath are challenging features of the hemispheric transducer for TUS. Instead, smaller transducers with a resulting larger focal spot are usually used for low intensity applications (Figure 4). Steering in depth can be achieved by annular arrays, while steering in 3D can be achieved with 2D arrays (Chaplin et al., 2018). Single element and annular array transducers are often used in small animal and cell culture studies, where plastic adapters are frequently used to couple the transducer to the head or medium (Tyler, 2011). Adapters add acoustic boundaries

that can change the shape and intensity of the ultrasound beam and must be considered during ultrasound exposure estimates as shown in (Ye et al., 2016).

4. Targeting the ultrasound beam within the skull

A primary technical challenge in all TUS procedures is targeting the focused sound to the region of interest. The distance between the intended focus and the actual focus is referred to as the target registration error (TRE), and the minimization of TRE has been the subject of the field of neuronavigation for many decades (Fitzpatrick et al., 1998). Placing an ultrasound transducer relative to the head is an analogous problem to placing a neurosurgical instrument and methodologies draw from the history of neuronavigation. In small animals, the ultrasound focus is typically placed based on prior knowledge of brain regions relative to landmarks on the head (ears, bregma, etc.). Targeting of the TUS beam becomes increasingly challenging in larger animals where the skull distorts and displaces the beam from the focus.

Optical tracking is a noninvasive neuronavigation method that has commonly been used for transcranial magnetic stimulation (Herwig et al., 2001; Cincotta et al., 2010; Ruohonen and Karhu, 2010) and increasingly for transcranial ultrasound (Kim et al., 2012a; Legon et al., 2018b; Wu et al., 2018; Yang et al., 2018, 2021; Chaplin et al., 2019; Phipps et al., 2019; Fouragnan et al., 2019; Verhagen et al., 2019). Optical tracking uses an infrared stereo camera to measure the position and orientation of reflective markers that are rigidly affixed to a tool, enabling the tool's location to be tracked in physical space (Kral et al., 2013). In a fiducial-based workflow, markers that are visible in a 3D imaging modality, such as CT or MRI, are placed on the patient and their physical positions relative to the camera are recorded using an optically tracked stylus. The fiducials are localized in a pre-acquired image space. The two sets of fiducial locations can be used to define a rigid transform so that tools with reflective markers can be tracked in real-time and projected into the image space (Labadie et al., 2005). By placing a tracker on the transducer, the position and orientation of the transducer and its free-field focus can be overlaid on pre-acquired images of the anatomy. Optical tracking occurs in real-time so the user can position the transducer during procedures which increases the range of targets that can be sonicated in a single procedure compared to rigidly fixed methods (FUS-Foundation, 2015). Studies in monkeys and rodents have reported TRE between the intended target and center of the acoustic focus of 2-3 mm (Kim et al., 2012a; Chaplin et al., 2019). The TRE is a function of all aspects of the neuronavigation system such as fiducial localization error, image voxel size, and image geometric distortion. Similar accuracy positioning of the estimated free-field focus is possible in humans, but the human skull can cause greater displacements of the focus potentially increasing the TRE.

5. Acoustic simulations in neuromodulation

Simulation of the wave propagation through the skull and in the brain that occurs after placing the transducer is an important supplement to neuronavigation. Acoustic simulations non-invasively correct for individual skull morphology for focusing precision, positional accuracy, reduction of

standing waves, and increasing target pressure amplitude (Kyriakou et al., 2014). The benefit of using simulations to correct for waveform distortion range from minor, e.g. when the wavelength is large compared to the skull thickness, to critical, e.g. when the wavelength is significantly smaller than the skull thickness. For example, a high fundamental frequency such as 500kHz corresponds to an acoustic wavelength of 3mm which is smaller than a typical cortical thickness. Since smaller wavelengths generate smaller focal spot sizes, it is also usually more desirable to increase the targeting accuracy in these cases. Low wavelengths, on the other hand, are more prone to generating disruptive standing wave patterns, especially in small heads.

Simulations use a map of the acoustic properties of an individual skull which is usually obtained via the conversion of a previously acquired CT to maps of density, speed of sound, and attenuation (Clement and Hynynen, 2002a, 2002b; Aubry et al., 2003; Jing et al., 2012; Pinton et al., 2012a, 2012b; Marsac et al., 2017; Robertson et al., 2017). Although this CT to ultrasound map conversion process can be challenging since the radiodensity is not directly equal to acoustic parameters (Robertson et al., 2017) and the resolution of CT scans may be too coarse to resolve acoustically relevant structures (Pinton et al., 2012a) mapping acoustic properties from CT is widely used. Images from ultrashort echo time (UTE) MRI (Miller et al., 2015) can also be used to estimate skull properties, the resultant ultrasound transmission and deviation into the brain. Efforts are underway to validate skull modeling using MRI and to measure the acoustic properties of skull bone as function of MRI parameters (Guo et al., 2019).

The wide variety of acoustic simulation approaches that have been used or developed for transcranial ultrasound propagation can be divided into ray tracing, angular spectrum, full-wave fluid, and full-wave elastic approaches, each with their own tradeoffs in terms of computational complexity and accuracy. In the simplest cases, CT scans of the skull can be segmented into average or effective speed of sounds and the phase correction can be calculated directly from the skull thickness (Clement and Hynynen, 2002b), using ray tracing software in commercial systems such as the ExAblate4000, or using phase projection (Pinton et al., 2012c). In 10 ex vivo skulls, it has been shown that this phase correction approach restores 76% of the focal peak of the non-aberrated case in the absence of the skulls as measured by hydrophones (Clement and Hynynen, 2002b). Ray tracing methods are extremely fast but do not account for diffraction or multiple reflections. Angular spectrum methods or methods that are based on the Rayleigh integral account for diffraction have been used (Clement and Hynynen, 2002a; Zeng and McGough, 2008; Vyas and Christensen, 2012) successfully and may be preferable in cases where the aperture of the transducer is small or other diffraction effects are important. To account for heterogeneities within the skull or the brain, full-wave solutions of the wave equation are used with time domain or pseudo-spectral methods in a fluid approximation (Pinton et al., 2009, 2012c; Jing et al., 2012; Treeby et al., 2012; Marsac et al., 2017) or in a fully elastic mode (Pichardo and Hynynen, 2007; Pinton et al., 2012a). These solvers, which are generally the most computationally costly, can include a high degree of complexity, including the skull trabecular microstructure, sophisticated attenuation mechanisms, standing waves, and mode conversion between longitudinal and shear modes, which are useful when calculating standing waves, propagation from shallow angles of incidence, and propagation through thick layers of the skull that contain complex microarchitecture.

Simulation tools can thus mitigate challenges with TUS by predicting them and the appropriate numerical tool must be chosen for a given challenge, including focal correction, prediction of skull heating, estimation of the pressure amplitude at the focus, the size and location of the focal zone, the magnitude of standing waves and other off-target effects, heating in the focal zone, etc. Currently, full simulations may not be feasible for many real time applications due to the computational time needed, but accelerating simulations is an active area of research.

6. Mapping ultrasound beams

In order to apply focused ultrasound through the skull it is important to be able to estimate the transcranial pressure field. Challenges in directly measuring the pressure in vivo necessitate methods for estimating the transmitted pressure distribution and for measuring effects of the pressure. Laboratory measurements can be made with hydrophones to assess the pressure output and distributions in water tanks in the free field or through ex vivo samples. Further experimental data can be collected using imaging methods to assess the effects of the TUS such as heating or displacement. MRI is widely used with TUS as it provides the ability to image heating due to thermal deposition or displacement from the acoustic radiation force.

The effects of the ultrasound beam on the tissue can be measured with MRI, which provides a direct measure of the beam location for a given experimental setup. MR thermometry has been widely used with clinical focused ultrasound ablation treatments to both localize the beam and monitor treatment (Meng et al., 2020). Multiple methods are used to measure temperature changes with MRI (Rieke and Pauly, 2008). The most commonly used method is based on the proton frequency shift, which measures phase changes in successive images induced by temperature changes, in turn resulting in changes to the local magnetic field. However, the use of MR thermometry has the potential to cause damage via excess heating following the absorption of ultrasound in the skull or brain, or to cause unintended neuromodulatory effects, since neuronal activity and temperature have been linked (Wang et al., 2016), and firing rates changes have been observed with even minor temperature changes (Boulant, 1974; Owen et al., 2019).

The beam position can also be measured though displacements induced in the tissue by the acoustic radiation force. When ultrasound propagates through tissue a force is applied in the beam propagation direction which can result in micron scale displacements (Sarvazyan et al., 2010). These induced displacements can be measured with MR acoustic radiation force imaging (MR-ARFI) using motion encoding gradients (Sarvazyan et al., 1998; McDannold and Maier, 2008). MR-ARFI localization can be performed with less than one degree of temperature rise and TUS intensities which are expected to be safe (Phipps et al., 2019; Ozenne et al., 2020). A safety study in sheep used a number of MR-ARFI sonications and then performed histology and did not detect significant evidence of damage (Gaur et al., 2020).

Methods to reduce the amount of TUS energy needed to localize the beam with MR-ARFI have been developed by reducing the number of sonications needed or improving the sensitivity of the imaging. Fast imaging methods like single shot echo planar imaging (Kaye et al., 2011) or keyhole acceleration (Paquin et al., 2013) allow for fewer sonications to be used when localizing the beam.

Optimization of the motion encoding gradients shape (Chen et al., 2010) and orientation (Phipps et al., 2019) allows for localization at lower TUS intensity by detecting smaller displacements in the tissue. Simultaneous MR thermometry and MR-ARFI can be performed to track the temperature rise during ARFI sonications to assess off-target heating (Auboiroux et al., 2012; Ozenne et al., 2020).

7. Mechanism of TUS

Understanding the aggregate mechanisms of ultrasound neuromodulation (excitatory or inhibitory) is critical for both informed experimental and therapeutic parameter selection. At present, there are three dominant mechanisms considered by the community: cavitation, temperature change, and mechanical deformation (Figure 5**)**. It is important to consider that these mechanisms can operate in parallel and that all neural subtypes and experimental paradigms likely have different sensitivities to various mechanisms. Thus, the parameters selected, and the nature of the target must be examined for the expected contribution of any given mechanism and explained accordingly.

It has been suggested that cavitation might be a prominent mechanism of TUS neuromodulation (Plaksin et al., 2014, 2016). Acoustic cavitation occurs when pressure falls below the vaporization point of the lipophilic zone of the membrane. This causes the oscillatory formation or bubbles inside the neuronal membrane. While there is little doubt that bubbles forming inside the cell membrane would cause neuromodulation through capacitance changes or fracture of the cell membrane, commonly used effective parameter space suggests that neural activity changes occur in its absence (Yoo et al., 2020). Because of the time required for vaporization and bubble formation to occur, increasing ultrasound frequency limits meaningful bubble growth before reversing the pressure sign. The pressure-frequency relationships to bubble radius have been examined in detail (Brennen, 2013). However, treatments purposefully using cavitation parameters—low frequency and high pressure and/or presence of injected large gaseous nuclei—have used this mechanism effectively for litho- and histotripsy, and blood-brain barrier opening (Tung et al., 2011; Kim et al., 2014b; Ramaswamy et al., 2015; Todd et al., 2018; Sukovich et al., 2019; Meng et al., 2021). Nevertheless, the lack of bubbles in typical ultrasound neuromodulation experiments observed through imaging and computational efforts has led researchers to explore alternative mechanisms.

Numerous studies have demonstrated modulation of neural activity in the mammalian brain with changes in temperature of as little as +0.1 °C (Owen et al., 2019). Although it is curious that the brain would be sensitive to changes less than its own natural fluctuation, it suggests that the brain may be continuously tuning its neural activity in response to local temperature (Wang et al., 2014). Because ultrasound waves are partially absorbed as they travel, ultrasound is a natural vector for delivering heat to tissue (Barnett et al., 1997). Numerous studies have shown reversible suppression of neural activity following ultrasound induced thermal rise. While our mechanistic understanding of thermal neural inhibition is rapidly advancing, there is growing evidence to support the role of increased potassium channels conductance, which reduces resting membrane

potential and, consequently, neuronal firing (Kubanek et al., 2016; Prieto et al., 2020). Some specific potassium channel subtypes examined in the context of ultrasound stimulation are TREK1,2, and K2P or TRAAK. Given the diversity of channel types that are at least moderately thermosensitive, a larger characterization of the brain and each region and its cell type profile will provide a deeper understanding of thermal neural suppression. Recent discoveries surrounding both warm and cold sensitive thermoregulatory neurons of the hypothalamus may help drive these larger studies (Abe et al., 2003; Tan et al., 2016).

Despite experimental and mechanistic evidence, the coincidence of thermal rise with other mechanical factors during ultrasound exposure leaves the role of thermal effects in ultrasound neuromodulation somewhat ambiguous. In response, a recent study made high precision temperature measurements in the thalamus of anesthetized rats and found that temperature increase produced by ultrasound was the best predictor of neural inhibition with obvious effects occurring at +0.5°C. Importantly, this correlate remained when other factors such as peak intensity and duty cycle were varied (Darrow et al., 2019). Although the narrow scope of thalamic inhibition under anesthetic state does not allow for broad application of this finding to other works, it strongly supports the role of temperature in TUS neural inhibition. However, a growing body of evidence also supports the role of mechanical force in ultrasound neuromodulation.

More recently, attention has shifted towards the mechanical interaction of TUS waves with the lipid membrane as a primary mechanism for neuromodulation; particularly to explain excitatory effects with limited increases in temperature. The theory generally states that the non-random mechanical deformation of the cell membrane leads to changes in both channel kinetics and membrane capacitance resulting in altered excitability. Although mechanosensation is a broadly studied feature of peripheral sensory systems (Reed-Geaghan and Maricich, 2011), mechanosensation has not readily been accepted for general neural response to ultrasound. This is possibly due to lower expression of relevant mechanosensors, and a less obvious need for mechanosensation in the brain. Physical displacement of the membrane by ultrasound has been measured using synthetic bilipid membranes, and directly observed in plated retinal slices (Rohr and Rooney, 1978; Prieto et al., 2013; Menz et al., 2019). These studies concluded that radiation force, or the transfer of momentum onto the membrane, is responsible for ultrasound excitation. While it is not clear how mechanical force exerted on a membrane alters channel kinetics, one model suggests that lipophilic lipid rafts are dispersed with low levels of mechanical force; this dispersion causes enzyme-substrate mixing and the production of mechanosensory channel ligands (Petersen et al., 2016). While there is no published evidence yet of ultrasound stimulation causing this mixing, the study showed that shear force generated by flowing solution over cultured cells produces substantial mixing (Petersen et al., 2016). This could be indirectly compared to compression force and resulting shear waves or more directly with acoustic streaming which may also play a role in ultrasound neuromodulation (Peng et al., 2021). The channels responsible for transduction of mechanical force into neural activity are under fierce investigation. Piezo1, a mechanosensitive channel expressed in the brain, is effectively activated by ultrasound in cultured cells (Coste et al., 2010; Prieto et al., 2018). In the same system, $Na_v1.2$ mechanosensitive channels were not activated by ultrasound but did change conductance in response to temperature. In an anesthetized mouse, TrpA1 (an astrocytic mechanosensitive Ca^{+2} channel) expression in the motor

cortex was found to be necessary for ultrasonic stimulation of tail movement, with the effect requiring calcium conductance (Oh et al., 2019). One recent exhaustive study found that ultrasound excitation of cortical culture neurons also requires calcium conductance and found that TRPP1/2, TRPC1, and TRPM4 ion channels are all partially responsible for the effect (Yoo et al., 2020). Another recent study found that TRAAK channels increased potassium conductance in response to low intensity ultrasound (Sorum et al., 2021). In contrast, increased temperature in the same preparation decreased TRAAK conductance suggesting that thermal effects would hinder rather than explain the modulatory effects of ultrasound. Collectively, it seems that a diversity of ion channels regulate ultrasound neuromodulatory effects through mechanical disruption of the membrane, and channel composition likely varies substantially across cell types. While nearly all mechanosensitive channels have also been identified as thermosensitive, ultrasound can seemingly activate these channels independent of any meaningful thermal shift.

TUS can be applied in either an online or offline approach. "Online effects" are measured during or immediately after TUS. "Offline effects", on the other hand, are measured minutes to hours, possibly even days, after the stimulation and presumably reflect structural and functional neuroplastic changes. The time course of offline effects of TUS on the nervous system suggests that it can induce long-term plastic changes beyond short term neuronal adaptation (Folloni et al., 2019; Fouragnan et al., 2019; Verhagen et al., 2019; Zeng et al., in press). These changes can occur at synaptic as well as non-synaptic sites in the neuron may result from alterations in the expression level or biophysical properties of ion channels in the membrane. TUS can activate mechanosensitive voltage-gated sodium and calcium channels, which in turn depolarize postsynaptic neurons to allow calcium influx through the N-methyl-D-aspartic acid (NMDA) receptors. The elevation of postsynaptic calcium has been considered as a critical precondition for inducing long-lasting changes in synaptic efficacy (Citri and Melanka, 2007). The involvement of NMDA receptors is supported by the finding that TUS to the thalamus of rats anesthetized with ketamine, as NMDA receptor antagonist, could shorten the time of arousal after administration of anesthesia (Yoo et al., 2011b). Another study revealed TUS can restore long-term potentiation (LTP) and memory in senescent mice, highlighting that TUS can modulate the function of NMDA receptors (Blackmore et al., 2021). In the same study, it was shown that TUS can increase or decrease several proteins associated with different functions including regulation of excitatory synapse development, and induction of LTP and long-term depression (LTD). A parallel experiment on the potential role of astrocytes, which are pressure sensitive, in mediating NMDA receptor signaling showed that ultrasound can open TRPA1 channels in astrocytes, leading to influx of calcium ions which in turn release glutamate that activates NMDA receptors in adjacent neurons (Oh et al., 2019). What remains to be understood, however, is how the brief ultrasound stimulation results in apparent sustained change in the function of ion channels, ultimately leading to LTP-like plasticity. Understanding the intracellular signaling cascades generated by TUS, therefore, should be the focus of future studies in characterizing its mode of action.

8. Indirect sensory effects of TUS

Another mechanism by which ultrasound may indirectly interact with the nervous system to drive neuromodulation is through its audible effects. While the fundamental frequencies typically used in ultrasound neuromodulation studies are far outside the hearing range of humans or animals (hearing range of humans: 15Hz-20 kHz, rats: 200Hz-90kHz, cats: 55Hz-77kHz) (Turner et al., 2005), early animal studies reported neuronal activity along the auditory pathway, including the auditory nerve, cochlear nucleus, and auditory cortex following TUS (Wever et al., 1958; Foster and Wiederhold, 1978). It was proposed that this hearing phenomenon was related to mechanical vibrations, presumably through bone conduction to the cochlea where they are detected (Foster and Wiederhold, 1978). Around the same time, such auditory effects had been also reported following electromagnetic pulse stimulation operating even at much higher frequencies (Frey, 1961). Nonspecific effects of ultrasound stimulation are not only limited to sensory side effects as other studies have demonstrated that unilateral motor cortex stimulation can cause bilateral motor responses involving bihemispheric interactions (Ye et al., 2016). Interestingly, targeting non-motor cortical regions closer to the cochlea elicited more robust motor responses than stimulating the motor cortex directly (Mehić et al., 2014; Ye et al., 2016), suggesting that ultrasound neuromodulatory effects in small animals might hinge on involvement of the auditory pathways.

To further understand the neurophysiological substrates underpinning ultrasound-induced sensorimotor responses, two studies investigated how widely used ultrasound neuromodulation parameters activate auditory pathways (Guo et al., 2018; Sato et al., 2018). Electrophysiological recordings of guinea pig primary auditory cortex (A1) revealed that ultrasound stimulation activates A1 indirectly and through an ascending cochlea fluid pathway (Guo et al., 2018). Moreover, the primary somatosensory cortex (SC1) was activated even when the stimulus was applied to the visual cortex. Both A1 and SC1 responses were diminished by removing cochlear fluid in both ears (Guo et al., 2018). In a parallel study, wide-field calcium imaging was used to assess large-scale neural responses to focused ultrasound with high spatiotemporal resolution in transgenic mice expressing the fluorescent calcium indicator GCaMP6s (Sato et al., 2018). The authors showed that ultrasound stimulation activated the auditory and sensorimotor cortex even when targeting ultrasound to the mouse visual cortex (Sato et al., 2018). Notably, the modulation frequency (PRF) used, 1500 Hz, is on the edge of the audible range of mice and could elicit an auditory response. Taken together, these studies raised the concern that acoustic or other cross-modal sensory responses confound the direct neuromodulatory effects of ultrasound stimulation applied to different regions of the brain, at least in small animals such as rodents.

Another study examined the mechanism underlying motor responses and showed that auditory brainstem responses were indeed elicited when ultrasound was applied to motor cortical areas in mice. The audible wideband acoustic frequency components were primarily due to the sharp rectangular envelope of ultrasound pulses or trains, and using a smooth envelope attenuated or eliminated audible components and auditory brainstem responses (Mohammadjavadi et al., 2019). Furthermore, the ultrasound pulse duration correlated with muscle response duration measured by electromyography (EMG), suggesting that evoked motor responses are not a mere result of stimulation of the peripheral auditory system. This conclusion was further supported by reproduction of the EMG responses in genetically deaf mice (Mohammadjavadi et al., 2019).

Despite the findings that auditory components of ultrasound may contribute to the neural or behavioral responses, there is strong evidence that neuromodulation can occur independent of auditory effects (Mohammadjavadi et al., 2019; Braun et al., 2020). For example, neuromodulation occurs in cultured neurons, retina, or brain slices which are isolated from any auditory systems (Tyler et al., 2008; Menz et al., 2013; Naor et al., 2016; Yoo et al., 2020). Neuromodulatory effects demonstrated in chemically or genetically deaf mice have also supported this notion (Sato et al., 2018; Mohammadjavadi et al., 2019). Moreover, site-specific effects such as ultrasound over the frontal eye field modulated saccadic behavior in monkeys (Deffieux et al., 2013; Wattiez et al., 2017) and ultrasound over the somatosensory cortex of humans provoked tactile sensation (Lee et al., 2015), support the notion that acoustic side effects are not the primary source of the neuromodulatory effects of focused ultrasound. Nevertheless, these effects should be considered in future human studies and adequate control experiments are needed to address this confound. A human study showed that auditory effects can be successfully masked using simultaneously applied audible stimuli (Braun et al., 2020). This study confirmed that participants could perceive the sound associated with TUS and the auditory effects were reflected in electroencephalographic (EEG) signals recorded simultaneously (Braun et al., 2020). When TUS was applied in conjunction with an audio waveform delivered to the participant via earphones, subjects were not able to distinguish in which trials TUS was applied based on the sound (Braun et al., 2020). The masking also successfully abolished TUS-induced auditory EEG signals.

Advances in modeling wave propagation have furthered our understanding of the mechanisms underlying audible components of ultrasound stimulation. It has been shown that acoustic pressure can induce significant propagation of shear waves outside the ultrasound focus using a finite element model of ultrasound wave propagation in the human skull (Salahshoor et al., 2020). Such waves could easily reach off-target structures such as the cochlea to produce audible sound. Furthermore, their models confirmed that ramped pulses of focused ultrasound resulted in much lower displacements than the sharp rectangular envelope (Mohammadjavadi et al., 2019; Salahshoor et al., 2020). These findings warrant further research on the effects of different stimulus envelopes in human studies.

Motor responses such as muscle twitches from ultrasound stimulation of the cortex have not been observed in humans or other large mammals, despite explicit attempts as part of larger studies (Legon et al., 2018b; Fomenko et al., 2020). This may be due to differences in skull size and thickness, and experimental conditions under which ultrasound is applied. For instance, experiments in rodents often involve full or partial anesthesia, head fixation in a stereotactic frame, and higher intensities of stimulation. It is also possible that the species-specific functional neuroanatomy of the motor system simply makes it easier to cause suprathreshold excitation in rodents compared to humans and other investigated large mammals.

In contrast to the relatively well-studied auditory confounds, TUS may also produce a tactile (somatosensory) sensation due to vibrations and/or thermal effects on the scalp and/or in the skull. While these sensory effects have not been systematically investigated, they have been anecdotally reported by several labs.

In summary, while sensory confounds of ultrasound stimulation deserve further comprehensive and systematic studies, effective solutions are already available, such as modification of the ultrasound wave envelope (Mohammadjavadi et al., 2019; Salahshoor et al., 2020) and application of masking noise (Braun et al., 2020) during sonication to minimize the effects of these confounding factors in the application of ultrasound for neuromodulation.

9. TUS for neuromodulation in animal studies

The vast parameter space of ultrasound neuromodulation protocols is still largely unexplored in biological systems. Accordingly, an exhaustive examination of combinations of parameters, or even single parameter series, would be costly, and the unknown risk profile of novel parameter combinations may not allow its assessment to be performed in humans immediately. Thus, preclinical animal experiments are an excellent and arguably necessary step for guiding human studies in parallel with accurate modeling and simulations studies to predict the efficacy of ultrasound effect and to promote reproducibility of results. Since the earliest ultrasound neuromodulation experiments in cats (Fry et al., 1958), animal models have played a critical role in demonstrating the safety and efficacy of stimulation parameters as well as in the investigation of its neuronal mechanism of action (cf. section 7).

9.1. Neural readouts

Various techniques have become available to measure the immediate consequences of ultrasound stimulation for brain activity and behavior. In animals, invasive electrophysiological recordings serve as primary readouts of TUS-induced neural activity and can provide spatiotemporally granular information about cell-type specific activity. Depending on the target area, somatosensory-, motor- and visual-evoked potentials (SEP, MEP, VEPs) have been successfully recorded and have provided insight into the efficacy and direction of TUS effects, i.e., net excitation or inhibition. A study in mice showed that hippocampal stimulation increased cortical spiking activity, as reflected in local field potential (LFP) recordings (Tufail et al., 2010). In contrast, in other studies with different stimulation protocols, hippocampal LFP recordings indicated both enhancement and suppression of neuronal activity (Rinaldi et al., 1991; Bachtold et al., 1998). Bidirectional neuromodulatory effects of focused ultrasound were first demonstrated in New Zealand white rabbits (Yoo et al., 2011a). In this exploratory application, a craniotomy was performed to allow for unimpeded sonication, and TUS was delivered to the primary motor and visual areas of the brain. Combinations of different PDs and PRFs were applied, and visible motor activity with corresponding electrophysiological responses from the limb contralateral to sonication were observed. In another study, extracellular recordings from the supplementary eye field of monkeys following sonication of the frontal eye field (FEF), which provides input to the SEF, has also demonstrated bidirectional modulation of neuronal activity (increase or decrease in activity following TUS) at the single-cell level (Wattiez et al., 2017).

As neurotransmitters are critical for translating electrophysiological responses into cell signaling, molecular analysis of TUS effects have also been performed. In one study, extracellular

neurotransmitters were sampled from rostral brain areas using microdialysis before, during, and after thalamus exposure to TUS (Yang et al., 2012). Extracellular glutamate concentration did not change, while γ-aminobutyric acid (GABA) was reduced upon sonication. In another study using the same sonication parameters, extracellular concentration of dopamine (DA) and serotonin (5-HT) increased upon sonication (Min et al., 2011b). Much remains to be discovered about the detailed mechanism underlying these changes in extracellular neurotransmitters, which can be influenced by (a) their rates of synthesis or release, (b) their removal from the synaptic cleft, and (c) their degradation rate. Therefore, visualization using imaging modalities sensitive to specific neurotransmitter activity was proposed for future studies (cf. section 11.2).

In comparison to electrophysiological and molecular methods, non-invasive measurements offer a unique basis of comparison to human studies, in which invasive methodologies are seldom available. These methods, such as EEG or functional magnetic resonance imaging (fMRI), are spatiotemporally less precise than the invasive electrophysiological methods. Nevertheless, they provide important insight into the large-scale effects of ultrasound neuromodulation. For example, resting-state fMRI has been used to assess offline TUS effects on the coupling between the stimulated area and other distant regions, presumably forming a neural network to serve specific functions (Yang et al., 2018; Folloni et al., 2019; Verhagen et al., 2019; Khalighinejad et al., 2020). These studies have shown that the stimulation of the target region increases its coupling with multiple cortical and subcortical areas anatomically or functionally connected with the target area. Notably, the effects of repetitive TUS are regionally specific. Each brain area can be characterized by a particular set of inputs and outputs, called a ‘connectivity fingerprint’. For example, sonication of distinct regions of the medial frontal cortex caused changes in each area's connectivity fingerprint, but only when sonication was applied to the area itself, not to a control region (Verhagen et al., 2019). A very similar pattern has been observed for the anterior cingulate cortex (ACC) and the amygdala, which are part of each other's connectional fingerprints (Folloni et al., 2019). Importantly, sonication of deep structures is possible without impacting the superficial cortex that lies in the path of the ultrasound beam. For instance, stimulation of the amygdala can be conducted without observing changes in the functional coupling of cortical areas around the superior temporal sulcus (Folloni et al., 2019). The regional specificity of TUS has received further support from a FDG (18-fludeoxyglucose) positron emission tomography (PET) study in rat brains (Kim et al., 2013). In this study, spatial increases in the glucose metabolic activity level were highly concentrated at the center of the sonication focus. Collectively, these methods may provide a proof of principle which will support future human studies.

9.2. Behavioral readouts

While the combination of neural activity recordings with TUS contributes significantly to our understanding of the origination of TUS neuromodulatory effects, it is crucial to examine whether these neural effects are coupled to relevant behavioral outcomes. In this regard, numerous studies have focused on stimulating the motor cortex in rodents, or the visuomotor system in monkeys, which typically leads to explicit behavioral manifestations and provide quantitative metrics of TUS effects (Tufail et al., 2010; King et al., 2013; Younan et al., 2013; Deffieux et al., 2018; Kubanek et al., 2020). In rats, TUS has been shown to impact the cranial nerve VI, leading to abductive eye

movement ipsilateral to the hemisphere that was sonicated (Kim et al., 2012b). In rodent studies, paw, hindlimb, tail, and whisker movements have been observed during TUS, lending further support to the regional specificity of TUS effects (Tufail et al., 2010; King et al., 2013; Younan et al., 2013). It should be noted that, while these studies have shown that adjustments to the positioning of the transducers over motor cortex within a subject could differentially lead to the activity of isolated muscle groups, they have failed to reliably generate fine grained topographical maps of mouse motor cortex (Tufail et al., 2010). Moreover, the observed motor responses were often bilateral although TUS was applied over one of the two motor cortices. Apart from the possibility that these evoked motor responses were not a mere result of stimulation of the motor cortex (see section 8), the likeliest explanation is that the spatial segregation of different cortical motor areas in the mouse brain are below the resolution limits of TUS (Tufail et al., 2010). It is also important to note that TUS-induced motor responses produce an EMG pattern similar to spontaneous muscle responses (Tufail et al., 2010) and that they may require the integration of stimulus amplitude over a time interval of 50 to 150 ms to then result in an all-or-nothing response, with response probability depending on stimulus strength and duration (King et al., 2013). This clearly distinguishes them from the immediate and highly synchronized EMG response pattern observed during the motor evoked potential (MEP) elicited by suprathreshold electric (TES) or magnetic stimulation (TMS) and likely reflects different mechanisms of generation.

Similarly, studies in awake and behaving primates found that a unilateral single TUS burst over the FEF, a cortical site controlling eye movement, increased the latency of voluntary saccades away from a visual stimulus when stimulation was applied to the hemisphere contralateral to the visual cue (Deffieux et al., 2013; Pouget et al., 2020). TUS over the FEF can also bias the monkeys' decisions in a two-alternative choice task suggesting that the stimulation can interfere with high-level decision-making circuits in the brain (Kubanek et al., 2020). In this vein, bilateral stimulation of the rostral medial prefrontal cortex alters the ability of monkeys to represent and translate cue information into behavioral choices during reward-guided decision-making tasks (Fouragnan et al., 2019; Bongioanni et al., 2021). Interestingly, although basal forebrain stimulation does not change which decision is taken, it does alter the timing of the decision (Khalighinejad et al., 2020).

Recent work in rodents has also demonstrated the feasibility of conducting TUS experiments in freely-moving animals (Lee et al., 2018). In this study, the authors developed a small TUS head mount attached to a hinged transducer to sonicate motor cortical areas of unanesthetized freely-moving rats. The stimulation yielded more diverse types of physical responses, such as chewing and head-nodding, with less variability in response rates across the animals compared to those reported in anesthetized rats. This emphasizes the state-dependency of neuromodulatory effects, which needs to be taken into account when interpreting the relation of specific TUS parameters and behavioral as well as neuronal outcome measures.

9.3. Examination of effective parameters

A longstanding question in neuromodulation is which fundamental frequency is ideal for achieving neural effects. In one study, a range of carrier frequencies spanning 250-600 kHz was examined for eliciting an EMG response to motor cortex stimulation (Tufail et al., 2010), showed that response probability for any given ultrasound intensity was higher at lower frequencies. These

findings were later confirmed by (King et al., 2013). Interestingly, a study measuring spike rate in the salamander retina demonstrated exactly the opposite: higher carrier frequencies required less intensity to achieve a neural response (Menz et al., 2019). The authors reasoned that membrane displacement from radiation force is key to neural activation, which is directly related to frequency. By performing an in-silico examination of effective ultrasound field size, the same group found that greater tissue volumes were recruited with the larger ultrasound beam profiles. Since lower frequencies create larger focal fields, this may explain why earlier studies found larger effect size at lower frequencies (Tufail et al., 2010; King et al., 2013). A recent study took special care to fix focal volume using dynamic mounted apertures and found that tactile peripheral nerve stimulation was greater at lower frequencies when stimulated volumes were matched (Riis and Kubanek, 2021). While this finding is generally applicable to all neural cell types, it is known that tactile neural structures are particularly sensitive to low modulation frequencies, which may overlap with natural frequencies generated by touch (Gavrilov et al., 1996). Given the contradictory nature of these findings, further research applying fixed field size at varying frequencies across various tissue types will be critical in reaching concrete conclusions.

In addition to fundamental frequency, animal studies showed that choosing an appropriate PRF also plays a vital role in the efficacy of neural circuits and behavioral modulations. In a behavioral study using C. elegans, the probability of successfully evoking a reversal behavior, a sudden turn while moving forward, is non-monotonically related to PRF with an initial increase with frequency from 30 to 100 Hz followed by a decrease with frequency at PRFs > 1 kHz (Kubanek et al., 2018). In a recent electrophysiological study, neuron-type-specific responses as a function of PRF were investigated through multi-channel extracellular recordings in rodent brains (Yu et al., 2021). While fast-spiking inhibitory neurons did not demonstrate significant changes in their spiking rate, excitatory neuron spiking activity increased substantially when PRF increased (Yu et al., 2021). The authors argued that the observed differences might be due to the distribution and type of ion channels in the neuronal cell membrane, morphology, size, etc. Future studies should consider examining PRF while holding the I_{SPPA} and I_{SPTA} intensities constant.

Beyond fundamental frequency and PRF, the stimulus repetition frequency (the frequency in which the pulse train is repeated), a third layer of temporal TUS protocol design, can affect the outcome. Examination of stimulus repetition at frequencies from 0.25 to 5 Hz showed that EMG motor response probability following motor cortex stimulation dropped as stimulus repetition frequency approached 5Hz (Tufail et al., 2010). Such a relationship is highly relevant to consider when designing both online and offline TUS protocols for neuromodulation.

Beside the temporal stimulation characteristics, ultrasound peak pressure and pulse duration are among the most critical features of short pulsed ultrasound, dictating the extent of both thermal and mechanical forces. The majority of ultrasound neuromodulation studies have at least some titration of either of these features, however, some have created more thorough dose response curves in their model systems. In C. elegans, there is a non-monotonic relationship between pulse duration, determined by duty cycle, and behavioral turning response to ultrasound; this may have been due to the onset of substantial thermal effects at higher duty cycles (Kubanek et al., 2018). A sigmoidal dose response curve to pressure peaking at ~1 MPa was also observed with fixed duty

cycle. Similar response curves have been observed for rat EMG response to motor cortex TUS and salamander retina spiking, albeit all studies found different peak pressures/intensities required (King et al., 2013; Menz et al., 2019). In these same studies, sonication duration examined in a collection of studies had a maximal effect between 100-200ms for a single continuous pulse. In cortical cultured neurons, the relationship between pulse intensity and duration appeared more linear with a maximum of 1MPa applied pressure and 500ms duration (Yoo et al., 2020). This may indicate lowered sensitivity to ultrasound in the absence of an integrated nervous system.

Importantly, the effective parameter space can be dramatically altered by the behavioral state of an animal. Depth of anesthesia can explain the variability of TUS induced neuromodulation and motor responses; high levels can completely suppress the TUS response (King et al., 2013; Younan et al., 2013). This reduction is likely explained by the pronounced direct network inhibitory effects of anesthesia. It is also worth considering the impacts of the reduction in body temperature associated with anesthesia, since ultrasound may act through thermosensitive channels (cf. section 7) (Caro et al., 2013). The superimposition of TUS and sensory inputs may also reduce the strength of each input, as demonstrated in human studies (Kahneman, 1968; Ide and Hidaka, 2013; Ryu et al., 2018). In line with this, while TUS led to a disruption of tactile stimulus-evoked fMRI BOLD responses in the targeted area, it directly activated the same area in the resting state (Yang et al., 2021). Thus, effective parameter comparisons should be considered carefully when differences in experimental paradigms exist, and a systematic evaluation of brain state-dependent TUS effects is desirable.

Appropriate parameter selection can also determine how long the neuromodulatory effects will last. For instance, electroencephalographic somatosensory evoked potentials (SEP) following 10 min application TUS to the sensory area of rats revealed that suppressive neuromodulatory effects lasted for more than 30 min after the sonication (Yoo et al., 2018). This duration is known to be sufficient for inducing initial long-term potentiation (LTP) or long-term depression (LTD)-like synaptic behavior (Castro-Alamancos et al., 1995; Malenka and Bear, 2004). Similar offline effects spanning from 10 min to more than 90 min have also been observed in pigs and monkeys (Dallapiazza et al., 2017; Folloni et al., 2019; Verhagen et al., 2019; Pouget et al., 2020). A recent in-vitro study showed that a 40s stimulation can induce an alteration of the physiological properties of the neuron for up to 14h without changes to intrinsic membrane properties or synaptic ultrastructure (Clennell et al., 2021). These findings provide important early evidence that TUS has the potential to induce long-term neural plasticity of the brain, a key feature required for developing therapeutic strategies.

9.4. Modeling human disorders with animal models

With growing understanding of effective methodology for studying ultrasound neuromodulation, preclinical examinations of human disorders are also on the rise. A neuroprotective effect of low-intensity ultrasound in a rat model of vascular dementia and aluminum-induced Alzheimer's disease has been reported (Lin et al., 2015; Huang et al., 2016). Specifically, ultrasound enhanced the levels of brain-derived neurotrophic factor (BDNF), an essential regulator of long-term memory, in the hippocampus and corpus callosum of the treated rats (Lin et al., 2015; Huang et al., 2016). These findings were in line with enhanced cognitive functions reported in mouse models

of dementia following whole-brain low intensity ultrasound (Eguchi et al., 2018). Furthermore, a stroke model has been examined by recording EEG during artificially induced stroke in mice. Cerebellar TUS was shown to normalize disrupted cortical oscillations and functional asymmetry between hemispheres after ischemic stroke (Baek et al., 2019). TUS application in disorders of consciousness has also been examined. Sonication of the ventral tegmental area (VTA) in mice under isoflurane-induced anesthesia has successfully aroused them from unconsciousness (Bian et al., 2021). The same study also reported that TUS reduces the recovery time from anesthesia in mice with traumatic brain injury. In the same light, another study had reported that TUS of the thalamus accelerated the emergence from anesthesia in rats (Yoo et al., 2011b). In examining TUS in parkinsonian disease, ultrasound was also applied to the subthalamic nucleus of mice administered the neurotoxin MPTP to generate a mouse model of Parkinson's disease (Wang et al., 2020). After TUS application, the mean beta power (13–30 Hz), a marker of parkinsonian-related activity, was significantly decreased. Additionally, by using chemically deafened mice, it was shown that TUS could decrease the beta band power independent of auditory confound (Wang et al., 2020). To explore the feasibility and potential mechanisms of TUS in depression, ultrasound was applied to the ventromedial prefrontal cortex (vmPFC) of rats and mice with depression-like features (Legrand et al., 2019; Zhang et al., 2021). The chronic unpredictable stress model was used to generate depression-like behaviors, and the vmPFC was chosen because of its role in emotion regulation. Low intensity ultrasound could significantly improve depression- and anxiety-related behavior by enhancing the BDNF and signaling pathways in PFC and brain areas far from the treatment zones (Legrand et al., 2019; Zhang et al., 2021). Among the more common therapies modeled in animals is the treatment of epilepsy. Epilepsy has been induced through various methods, including kainic acid injections, electrical kindling, and epileptogenic drugs. Almost ubiquitously, chronic pulse repetition reduced seizure intensity and event probability, or a behavioral proxy of epilepsy (Min et al., 2011a; Hakimova et al., 2015; Zou et al., 2020).

10. TUS for neuromodulation in human studies

Rigorous experiments using different animal models paved the road for safely migrating TUS application to human brains. Importantly, like other non-invasive brain stimulation (NIBS) techniques, TUS can be applied in either an online or offline approach. "Online effects" are measured during or immediately after stimulation to assess either the direct neural response to suprathreshold stimulation or subthreshold modulation (i.e., facilitation or inhibition) of ongoing neural activity. "Offline effects", on the other hand, are measured minutes to hours, possibly even days, after the stimulation and presumably reflect structural and functional neuroplastic changes. It is important to note that online and offline effects can overlap in some situations, for example when repeated application of online stimuli leads to a concurrent build-up of offline effects over time, thereby confounding the measurement of online effects for later trials. Outcomes used in TUS studies so far have mirrored attempts in other NIBS fields, and span across neurophysiological, behavioural, and clinical measures. In fact, the emerging field of TUS for neuromodulation in humans will greatly benefit from drawing on experiences with transcranial

magnetic stimulation (TMS) and low-intensity transcranial electric stimulation (tES), trying to translate experimental approaches, intervention protocols, and dependent measures across NIBS techniques. This approach is facilitated when using the same well-established measures across fields for assessing corticospinal excitability, such as the motor evoked potential (MEP). Moving forward, well-known issues such as inter-subject variability in effective 'dosing' (here including differences between intra- and extra-cranial intensity due to skull attenuation), and intra-subject variability due to homeostatic metaplasticity and brain state-dependency of effects must be addressed.

10.1. Online Evoked Effects

The most powerful demonstration of the effectiveness of TUS as a neuromodulation technique would be to cause perceptually and behaviorally relevant neural activity. Unfortunately, unlike TMS, there has been no report showing that TUS is able to evoke motor responses or associated MEPs in humans. However, several studies investigated whether TUS of the sensory cortices can evoke immediate neural responses (e.g, in EEG or fMRI) as well as explicit conscious sensations. Online TUS (f_0=250 kHz, PRF=500 Hz, DC=50%, stimulus duration (SD)=0.3 s, PD=1 ms, free field I_{SPPA}=3 W/cm^2) of the hand region of the primary somatosensory cortex (S1) has led to sonication-evoked potentials in the EEG, that mimicked the classical SEP generated by electric median nerve stimulation (MNS) (Lee et al., 2015). Despite this similarity, subtle differences between TUS- and MNS-evoked potentials in sensory cortex were observed, such as the absence of very short-latency evoked components following TUS, which may relate to the absence of an afferent signal (Lee et al., 2015). The estimated I_{SPPA} values provided in this section have been measured in water tanks in the free field, hence, they might differ substantially from true values at the target site based on individual bone attenuation (cf. section 2). Another study by the same group demonstrated the feasibility of using multiple transducers to probe the causal role of multiple brain areas in mediating particular sensory, motor, or cognitive functions (Lee et al., 2016a). Here, sonication of the secondary somatosensory area (S2) alone (f_0=210 kHz, PRF=500 Hz, DC=50%, SD=0.5 s, PD=1 ms, free field I_{SPPA}=35 W/cm^2), or in conjunction with the ipsilateral S1, induced the perception of tactile sensations in the contralateral hand. Simultaneously stimulating multiple areas in a spatially restricted manner empowers researchers to study how high-level perceptual, motor, or cognitive functions are mediated by large-scale networks. Potentially, different network nodes may be up- or downregulated separately by means of different TUS protocols. However, the specific parameter combinations that effectively determine bidirectional excitability changes are yet to be established.

TUS can be safely combined with either fMRI or EEG to assess the remote effects of TUS. Sonication of the primary visual cortex (V1) with eyes closed (f_0=270 kHz, PRF=500 Hz, DC=50%, SD=0.3 s, PD=1 ms, free field I_{SPPA}=16.6 W/cm^2) not only increased the fMRI blood oxygenation level dependent (BOLD) signal in V1 and an associated down-stream network of cortical and subcortical areas but also evoked EEG potentials similar to those observed during photic stimulation (Lee et al., 2016b). While photic stimulation using flickering checkerboard stimuli activated only a few nodes of the visual system (including V1, fusiform gyrus, and lateral geniculate nucleus of thalamus), TUS activated many more brain areas such as different parts of

the cerebellum, other nuclei of thalamus, and a few frontoparietal areas suggesting that TUS has had more widespread effects and engaged other circuitries beyond the visual pathway such as those involved in attention or movement control (Tehovnik et al., 2003).

TUS of V1 was also able to induce the perception of phosphenes in more than half of the subjects (Lee et al., 2016b). Surprisingly, the reported phosphenes occurred diffusely over the entire visual field without a precise retinotopic arrangement, a finding that is in contrast to TMS-induced phosphenes (Kammer, 1999). This finding suggests that the cigar-shaped TUS focus and imperfect targeting have caused the ultrasound beam to co-stimulate extrafoveal regions of downstream areas such as V2/V3, in addition to the central visual field representation of V1. Paralleling TMS for phosphene induction, future TUS studies should systematically move the transducer across the cortical surface while documenting the nature and location of the induced phosphenes to elucidate the neural substrate of TUS-induced phosphenes and advancing it as a tool to study the retinotopic organization of the visual cortex. Furthermore, depending on the intensity and experimental conditions, TMS can also induce a blind spot (scotoma) experience in the visual field (Murd et al., 2010), a phenomenon yet to be investigated using TUS. In summary, while suprathreshold excitation and resulting evoked neural responses and sensations seem possible, these TUS effects still need to be replicated across laboratories and studied in more detail.

10.2. Online Modulation

Besides this potential to evoke suprathreshold neural activity (similar to TMS), TUS is also (or even more so) able to produce subthreshold modulations of ongoing neural activity that was produced in response to a suprathreshold sensory stimulus or associated with the generation of a specific behavioral output (possibly comparable to the subthreshold modulatory effects of transcranial direct current stimulation, tDCS). In their seminal study, Legon et al., (2014) demonstrated that TUS (f_0=500 kHz, PRF=1000 Hz, DC=36%, SD=0.5 s, PD=0.36 ms, free field I_{SPPA}=23.9 W/cm^2) focally applied to S1 can attenuate the amplitude of somatosensory evoked potentials (SEPs) and cortical oscillations induced by MNS. These modulations were accompanied by lowered perceptual detection thresholds (i.e., increased performance), as measured using two-point and frequency discrimination tasks. Notably, these effects were absent when applying sham TUS or targeting brain regions 1 cm posterior or anterior to S1. A follow-up study by the same group with the same parameters showed that in addition to the amplitude of event-related brain oscillations, S1-TUS also influenced phase properties of both spontaneous (prior to MNS) and induced oscillations (following MNS) in a spatially specific manner (Mueller et al., 2014). These effects included alterations in phase distribution of both ongoing and early induced beta oscillations, and phase rate of spontaneous beta and gamma oscillations (Mueller et al., 2014).

The neuromodulatory effects of TUS on SEPs were further investigated by leveraging its ability to target deep structures such as the thalamus. Sonication of the ventroposterolateral (VPL) nucleus of thalamus, a sensory nucleus that projects to the S1, (f_0=500 kHz, PRF=1000 Hz, DC=36%, SD=0.5 s, PD=0.36 ms, free field I_{SPPA}=14.5 W/cm^2) attenuated the P14 SEP component (a positive peak in the EEG signal at around 14 ms following MNS) and decreased the participants' ability to perform difficult tactile threshold judgments (Legon et al., 2018a), a finding in contrast

to the enhanced tactile perception observed during sonication of S1 (Legon et al., 2014). However, this seeming contradiction may indeed be just another evidence for the region-specificity of TUS effects. It also suggests that TUS is not simply disrupting information flow from the periphery to S1, but it may instead involve more complex mechanisms depending on the anatomical and functional properties of the stimulated areas, including their connectivity with the rest of the brain.

While TUS-mediated modulation of sensory evoked potentials like the SEPs has proven fruitful for demonstrating the efficacy of TUS to modulate externally evoked neural activity and behaviorally relevant sensory processing, attention has recently shifted to the motor cortex, as here the mechanistic principles of modulatory TUS effects can be studied through the lens of the well-established TMS evoked motor response and MEP (cf. section 11.5). This is particularly informative as it links the novel field of TUS for neuromodulation in humans to the existing body of literature on TMS effects on human motor cortical and corticospinal excitability. Using this combination, it has been demonstrated that TUS, with the identical set of parameters used in the S1 experiments (Legon et al., 2014), reduces the amplitude of single-pulse TMS-evoked MEPs and attenuates intracortical facilitation measured by a paired-pulse TMS protocol (Legon et al., 2018b). While TUS caused effective suppression of motor corticospinal excitability during M1 sonication, it also reduced response times during a visuomotor task. Systematically varying sonication parameters (f_0=500 kHz, PRF=200,500,1000 Hz, DC=10,30,50%, SD=0.1-0.5 s, PD=0.5-0.6 ms, free field I_{SPPA}=9.26 W/cm^2), (Fomenko et al., 2020) showed that TUS suppresses MEPs more effectively at longer sonication durations (in a dose-dependent manner) and shorter duty cycles. It should be noted that for a constant I_{SPPA}, lowering the duty cycle leads to reduction of the I_{SPTA}, thus future studies need to specify if MEP suppressions are solely due to a shorter duty cycle, lower I_{SPTA}, or both. Again, as in (Legon et al., 2018b), these suppressive effects were accompanied by a facilitation in behavioral performance, i.e., a shortening of response times. It remains unclear how a suppression of corticospinal excitability and a facilitation of motor response times are related, but peripheral sensory confounds related to transducer activation may play a role in priming of action, and reduction of reaction time (Braun et al., 2020; Fomenko et al., 2020; Xia et al., 2021).

While the majority of human TUS studies seem to report inhibitory effects, two recent studies suggest that TUS may also be able to facilitate cortical activity (Yu et al., 2020; Liu et al., 2021). Movement-related cortical potentials (induced by a right foot pedaling movement) increased at both EEG sensor and source levels when TUS (f_0=500 kHz, PRF=300,3000 Hz, DC=6,60%, SD=0.5 s, PD=0.2 ms, free field I_{SPPA} =5.90 W/cm^2) was concurrently transmitted to the primary leg motor area, with higher PRFs (3000 compared to 300 Hz) facilitating this effect (Yu et al., 2020). The same group also showed that TUS of S1 (f_0=500 kHz, PRF=300 Hz, DC=6%, SD=0.5 s, PD=0.2 ms, free field I_{SPPA} =5.64 W/cm^2) enhanced spatiotemporal EEG responses in sensory cortical areas during a sensory discrimination task (Liu et al., 2021). In line with (Legon et al., 2014), this study showed that S1-TUS could enhance sensory discrimination capability with a higher percentage of correct responses. However, (Legon et al., 2014) related this finding to increased neural inhibition (reflected in decreased SEP amplitudes), whereas (Liu et al.,

2021) linked it to increased local excitation (reflected in increased spatiotemporal EEG responses). While these different findings of inhibitory vs. excitatory TUS effects in S1 may be explained by differences in ultrasound parameters, it also highlights that the relationship between cortical excitability and behavioral performance is complex.

Opposite effects of TUS on BOLD signal increases vs. decreases have also been observed in simultaneous TUS-fMRI experiments. One study for example reported that TUS (f_0=500 kHz, PRF=1000 Hz, DC=36%, SD=0.5 s, PD=0.36 ms, free field I_{SPPA}=16.95 W/cm^2) increased the BOLD signal activation volume of the M1 thumb representation (Ai et al., 2018), while sonication (f_0=650 kHz, PRF=10,100 Hz, DC=5%, SD=30 S, PD=0.5,5 ms, free field I_{SPPA}=14.4 W/cm^2) of the globus pallidus (GP) caused local and remote decreases in the BOLD signal (Cain et al., 2021b). When interpreting these findings, one needs to keep in mind that BOLD fMRI is not able to distinguish excitatory and inhibitory effects at the electrophysiological level (Logothetis, 2008) and that BOLD signal differences vary with the specific experimental design.

It should be noted that TUS, like any other NIBS technique, is state-dependent, i.e., its neural and behavioral effects depend on the history of neural activity as well as the current level of neuronal excitability, especially at the immediately targeted brain area (Ziemann and Siebner, 2008; Bergmann, 2018). State-dependency can be utilized by exposing the neural system to a stimulus for a short time (Churchland et al., 2010) or even repeatedly to induce neural adaptation (Silvanto et al., 2007; Silvanto and Pascual-Leone, 2008). Deliberately or involuntarily inducing a certain brain state before or during TUS may thus affect the efficacy of its neural and behavioral effects and hence their reproducibility across laboratories.

It should be noted that some studies did not include an active sham control or proper auditory masking. Therefore, it is not clear to what extent peripheral co-stimulation confounds (auditory or somatosensory stimulation, cf. section 8) may have contributed to online effects of TUS in those studies. An example of an active sham control is stimulation of an adjacent area (Legon et al, 2014). Careful assessment of the audibility of TUS can lead to design of appropriate auditory masking method (Braun et al, 2020).

10.3. Offline Modulation

A key application of NIBS in general is to induce excitability changes in the targeted brain region or network that outlast the stimulation itself, either with the intention to modulate performance during a subsequent task in cognitive neuroscience experiments (Bergmann and Hartwigsen, 2021), or with the intention to produce more long-lasting changes during therapeutic interventions (McClintock et al., 2018; Rapinesi et al., 2019). Also, offline TUS can be used to elucidate brain-behaviour relationships and has many potential clinical applications. The major advantage of TUS is its high spatial precision and its ability to reach deep brain structures that are currently accessible only by invasive deep brain stimulation (DBS).

There are very few reports of TUS in patients with neurological or psychiatric disorders. Studies so far have shown the promise of clinical applications in disorders of consciousness (Monti et al., 2016; Cain et al., 2021a) and pain (Badran et al., 2020) by targeting the thalamus, and in the context

of emotion regulation and depression by targeting the fronto-temporal cortex (Reznik et al., 2020; Sanguinetti et al., 2020). The first study of clinical application of TUS was an open labelled study in a 25-year-old man in a minimally conscious state due to traumatic head injury (Monti et al., 2016). The patient emerged from minimally conscious state three days after sonication of the right thalamus for 30 s, repeated 10 times, (f_0=650 kHz, PRF=100 Hz, DC=5%, SD=30 S, PD=0.5 ms, free field I_{SPPA}=20 W/cm^2) under MR guidance and no side effects were observed. In a subsequent unblinded study, three patients with chronic disorder of consciousness ranging from 14.5 to 66 months after injury received two sessions of MR guided TUS of the left thalamus with parameters similar to the previous study (Cain et al., 2021a). Two of the three patients had improved behavioral responsiveness, but one patient regressed after three months. (Badran et al., 2020) used a similar protocol but with a lower PRF to sonicate the right anterior thalamus (f_0=650 kHz, PRF=10 Hz, DC=5%, SD=30 S, PD=5 ms, free field I_{SPPA} =14.39 W/cm^2) for two 10-min sessions and induced antinociceptive effects (thermal pain sensitivity was significantly attenuated) in healthy individuals. Of the two studies by the same group, targeting the right fronto-temporal cortex, one study applied TUS (f_0=500 kHz, PRF=40 Hz, DC=0.26 %, SD=30 S, PD= 65μs, free field I_{SPPA}=14 W/cm^2) in five daily sessions over 7 days in 24 college students with mild to moderate depression, which were randomly assigned to active or sham TUS (Reznik et al., 2020). While there were no significant differences in the depression scores between the real and sham TUS groups, trait worry scores decreased in the active group and increased in the sham group. The other study (Sanguinetti et al., 2020) (f_0=500 kHz, PRF=40 Hz, DC=0.26%, SD=30 S, PD= 65μs, free field I_{SPPA}=54 W/cm^2) examined the underlying neurophysiological changes of the same protocol but at higher intensities in healthy participants and showed a decrease in functional connectivity in resting state networks, accompanying an improvement in global effect. The aforementioned studies include a combination of proof-of-principle studies in healthy adults and patients with limited sample sizes and often without control conditions. The clinical use of TUS for neuromodulation in humans is still in its early days, and more research is necessary before TUS can be incorporated into routine clinical practice. In addition to the need for larger controlled studies, the underlying neurophysiological changes leading to the observed symptom changes remain largely unknown, and only a small subset of the vast TUS parameter space has been systematically explored. Offline TUS protocols will likely benefit from attempts to conceptually translate successful protocols from other NIBS techniques, in particularly repetitive TMS (rTMS), e.g., the neurophysiologically well-grounded theta burst stimulation (Huang et al., 2005). A theta burst patterned TUS protocol (tbTUS) that produced consistent increase in motor cortical excitability in healthy human subjects for at least 30 min after 80 s of stimulation was introduced recently (Zeng et al., in press). These data suggest that tbTUS modulated both inhibitory and excitatory intracortical circuits, as measured by the paired-pulse TMS protocols of short-interval intracortical inhibition (SICI) and intracortical facilitation (ICF). In contrast, regularly patterned TUS, sham TUS, and occipital tbTUS had no effect on motor cortical excitability (Zeng et al., in press) Other offline protocols (f_0=250 kHz, PRF=10Hz, DC=30%, SD = 40s, PD=30 ms, free field I_{SPPA}= 18.8 to 64.9 W/cm^2) that successfully modulated functional connectivity and behavior in non-human primates (Folloni et al., 2019; Fouragnan et al., 2019; Verhagen et al., 2019) have applied higher I_{SPPA} and I_{SPTA} than those used in human studies so far and must thus be introduced carefully in humans.

Repeated administrations of repetitive TMS and tDCS are effective treatments of some brain disorders (Lefaucheur et al., 2020). Since studies in humans (Zeng et al., in press) and non-human primates (Folloni et al., 2019; Fouragnan et al., 2019; Verhagen et al., 2019) have demonstrated offline effects of TUS for 30 minutes or longer, which are of similar or greater extent compared to repetitive TMS (Chen et al., 1997, Huang et al., 2005) and tDCS (Nitsche and Paulus, 2000), repeated applications of TUS can be investigated as treatment for neurological and psychiatric disorders with the potential advantage of more focal stimulation and ability to stimulate deeper brain areas compared to currently available methods.

Some studies attempting TUS for neuromodulation in humans have utilized (modified) diagnostic ultrasound devices in the absence of dedicated low-intensity focused ultrasound systems. However, diagnostic ultrasound for imaging and TUS for neuromodulation rely on different mechanisms and require different hardware. Diagnostic ultrasound devices produce unfocused beams targeting larger brain volumes than focused TUS. Moreover, these devices usually use continuous waves and operate at lower power but much higher frequencies than TUS – above 1 MHz and up to 15 MHz. This is relevant, as attenuation through the skull increases with increasing ultrasound frequency (Pichardo et al., 2011). Nonetheless, several studies have reported behavioral and neural changes using diagnostic ultrasound for neuromodulation. These include improvement of subjective mood in patients with chronic pain (Hameroff et al., 2013), increased motor cortex excitability (Gibson et al., 2018), increased visual percepts (Schimek et al., 2020), and increased excitability of brainstem circuits as measured by the trigeminal blink reflex (Guerra et al., 2021). These effects broadly differ from focused TUS in that such protocols with diagnostic ultrasound devices appear to induce increases rather than decreases in cortical excitability, a difference that requires systematic investigation. Another sonication technique, called transcranial pulse stimulation (TPS), using diagnostic ultrasound devices and applying ultrashort pulses rather than continuous waves, has also been used in Alzheimer's disease therapy, reportedly improving neuropsychological scores lasting up to three months in an uncontrolled pilot study (Beisteiner et al., 2020). Since the use of diagnostic ultrasound devices for producing therapeutic neuromodulatory effects is just being investigated and their modus operandi differs from that of focused TUS, a thorough assessment and comparison of their respective safety parameters is needed.

11. Considerations for combining TUS with MRI, proton magnetic resonance spectroscopy (H-MRS), TMS and EEG

Similar to other NIBS technique, the effects of TUS on cognitive functions can be accessed via perceptual reports (e.g., of phosphenes or tactile sensations) and behavioral task performance (accuracy and response time), while the assessment of the mediating neural effects requires central or peripheral measurement of the brain response to TUS. Unlike TMS, TUS of the human motor cortex (at currently applied intensities) cannot produce measurable motor responses in the periphery, even though the induction of paw, whisker and tail movements are possible in rodents, and there are only few reports of TUS-induced phosphenes and tactile sensations in humans (Lee et al., 2015, 2016b). It is therefore crucial to measure TUS effects on brain activity directly.

Fortunately, TUS can be combined with a variety of neuroimaging (e.g., fMRI, rsfMRI, MRS, diffusion MRI) and electrophysiological (e.g., EEG, Magnetoencephalography (MEG), EMG) methods as well as other NIBS techniques (e.g., TMS) to assess both online effects, during or within seconds after TUS, and neuroplastic offline effects, that outlast the stimulation by minutes to hours. While EEG/MEG and fMRI can only detect correlates of peri-synaptic activity with complimentary strength regarding their temporal and spatial resolution, they cannot distinguish between excitatory and inhibitory contributions. However, TMS-EMG can be used to measure corticospinal excitability, and paired-pulse TMS-EMG protocols can shed some light on inhibition and facilitation in intracortical circuits. For a precise mapping of TUS-related neural activity changes to the estimated focus of stimulation, it is highly recommended to use a priori simulations of the sonication beam (based on CT or surrogate MR bone imaging) in combination with MR-guided neuronavigation. Together, these neuroimaging and neurostimulation techniques can help to assess the neural activity directly evoked by TUS as well as the TUS-induced online and offline modulation (facilitation or inhibition) of evoked or ongoing neural activity. Each technique is sensitive to different aspects of the neural response affected by TUS and possibly also to different neuron populations. The technique of choice thus depends on the respective research question.

11.1. fMRI and rsfMRI

fMRI detects whole-brain activity changes associated with blood flow with high spatial resolution, and can be measured while a task is being performed or while the participant is at rest (rsfMRI). Combining neuroimaging and neuromodulation, a “perturb and measure” approach (Paus, 2005), allows detailed causal inference of neural activity and thus provides insights into the function of specific brain regions, their functional interaction with other areas in distributed networks and ultimately their relation to cognitive mechanisms (Bergmann et al., 2021; Bergmann et al., 2016). Moreover, concurrent TUS-fMRI or -rsfMRI enables characterization of the impact of neuromodulation on brain activity and importantly allows us to assess the duration of these effects.

To date, TUS has been simultaneously combined with fMRI at both 3T and 7T field strengths in several studies in healthy humans. As the acoustic energy can be focused into localized areas - in the order of a few millimeters - studies combining TUS-fMRI can efficiently target highly specific regions, for example finger somatotopy in the primary motor hand area (Lee et al., 2015) or single nuclei in the basal ganglia (Ai et al., 2016; Cain et al., 2021b). These studies have shown that concurrent TUS-fMRI can increase the BOLD signal in sonicated regions (Lee et al., 2016b; Ai et al., 2016; Ai et al., 2018) with the exception of one study targeting the basal ganglia (Cain et al., 2021b). Depending on the aim of the study and the choice of TUS parameters and protocols, one may observe local changes in BOLD response amplitude at the target site (Yoo et al., 2011a), downstream effects in functional connectivity in monkeys (Folloni et al., 2019; Verhagen et al., 2019; Cain et al., 2021b), and volume changes of clusters expressing significant BOLD responses (Ai et al., 2018). All studies in humans to date have focused on the neural activity directly evoked by TUS in the targeted tissue, i.e., participants were resting while fMRI was recorded. Future studies might examine how TUS disrupts or modulates task-related BOLD responses and associated cognitive processes.

In addition to the standard protocols that have to be considered when using medical electrical equipment in an MR environment (ECSS 60601-1-2; ICNIRP, 2004; IEC, 2007), it is advisable to keep the following in mind to ensure an effective and safe use of concurrent TUS-fMRI. First, standard TUS transducers will not be appropriate as they contain lead zirconate titanate for the piezoelectric element. This can produce large susceptibility artefacts in the MR images. The transducers' size might also not provide the necessary degree of freedom for placement within the restricted MR environment, in particular when using conventional multi-channel head coils. Novel, TUS-optimized RF coil arrays would thus be desirable to increase SNR and maximize flexibility of transducer positioning, similar to what has recently been developed for concurrent TMS-fMRI (Navarro de Lara et al., 2017; Navarro de Lara et al., 2015). Even with an MR-conditional TUS transducer, the susceptibility artefacts will not be entirely eliminated and thus, careful shimming is required to be able to detect cortical activity directly under the transducer. On top of shimming strategies, optimal MRI parameters will need to be examined to maximize signal detectability, especially pulse sequence selection (i.e., GRE vs. spin-echo sequences). Additionally, any setup potentially leading to temperature changes (SAR levels, use of specific RF-transmit coils, or use of high static magnetic field strengths) should be monitored throughout the measurements to avoid potential heating of biological tissue (particularly below the transducer). Therefore, it is advisable that all new TUS-fMRI protocols should first be tested during phantom measurements. In addition, before starting with the actual measurement, several test pulses at the experimental intensity in the scanner environment need to be applied. This will allow to assess comfort with respect to 1) the auditory stimulation/auditory mask with adequate hearing protection, 2) the TUS position (when there is high pressure of the TUS transducer against the head, small cushions at the pressure point can help to distribute the weight), 3) the pulse sensation and 4) whether the TUS is stably mounted (avoid cable loops in the MR and trip hazards on the ground by securing all cables). Finally, it is likely that TUS will evoke extraneous BOLD activity in the auditory pathways, which will need to be controlled as a confounding factor (cf. section 8).

11.2. H-MRS

Proton magnetic resonance spectroscopy (^{1}H-MRS) is an in vivo technique that non-invasively measures molecular concentrations of metabolites in brain tissues. Spectra can be measured within single regions of interest, known as single-voxel spectroscopy (SVS), or across multiple voxels in two or three dimensions, known as chemical shift imaging (CSI). SVS might be more suited to measure focal effects at the TUS target, while CSI might be used to measure biochemical changes over a range of regions within and distal to the TUS focus. Of particular interest when using ^{1}H-MRS with a NIBS technique is the ability to quantify levels of excitatory (glutamate) and inhibitory (GABA) neurotransmitters in relation to the NIBS-induced neuromodulation. ^{1}H-MRS has been combined with other NIBS techniques such as TMS and tES, where changes in excitatory and inhibitory neurotransmitter concentrations have been detected following neuromodulation (Bachtiar et al., 2015; Cuypers and Marsman, 2021). It is worth noting that MRS cannot distinguish between extra- or intra-cellular metabolites, and the indirect measurement of neurotransmitter concentrations may not reflect synaptic activity, so drawing conclusions about the mechanism of action of NIBS-evoked excitation or inhibition may be difficult. To date (July 2021), a PubMed

search for studies combining MRS and TUS has yielded no results. However, the combination of MRS with TUS, in a similar way to its combination with other neuromodulatory techniques, has the potential to provide insights into the metabolic and biochemical mechanisms underlying TUS neuromodulation.

In addition to the practical considerations for combining TUS and fMRI mentioned above, combining TUS with MRS has some additional caveats. While neuronavigation of the TUS transducer is also highly beneficial for concurrent TUS-fMRI, it is obligatory for TUS-MRS to ensure overlap between the MRS voxel and the TUS focus, since off-target effects would not be detected. Molecular characterisation with ^{1}H-MRS generally suffers from low signal to noise ratio, which necessitates large voxels and long acquisition times. Voxels are often best sampled from deep cortical or subcortical regions (away from the skull and brain/air interfaces). Regions where the scanner B_0 field is inhomogeneous will be difficult to shim. Even with precise overlap, MRS voxels will often be much larger than the TUS focus – they can range from subcentimetric to several tens of cubic centimeters, depending on homogeneity of the region of interest, while TUS foci are often in the millimetric or sub-millimetric range. The voxel size and orientation should be aligned with the trajectory of the TUS beam to maximize overlap. Since MRS acquisition requires several minutes, it may be more suited for offline protocols or would need to be measured over the entire duration of multiple TUS deliveries in an online protocol.

11.3. Other MRI-related neuroimaging techniques

The combination of TUS with other neuroimaging techniques such as diffusion MRI (dMRI) and arterial spin labelling (ASL) allows the assessment of TUS-induced changes in brain microstructure and absolute changes in cerebral blood perfusion, respectively. While dMRI may be best suited for offline TUS, ASL can also assess immediate TUS-evoked changes in blood perfusion online. In a recent study, ASL revealed local and remote perfusion decreases both during (online) and following (offline) the sonication (Cain et al., 2021b). To date, there are no published neuroimaging studies looking at changes in structural plasticity related to TUS, but previous studies have shown that dMRI was able to capture changes in structural plasticity over short timescales after training or learning tasks (Sagi et al., 2012; Hofstetter et al., 2017; Brodt et al., 2018). It is thus likely that offline TUS may be able to induce structural plasticity changes in and around the targeted region that can be measured with dMRI. Finally, as discussed in section 6, MR-ARFI pulses sequences can be used concurrently with TUS to localize the acoustic focus prior to TUS procedures, by measuring the micro displacement caused by TUS. MR-ARFI-derived displacement measurements have been validated in small animals and in NHP studies, but not yet in humans.

11.4. EEG

Given its superior temporal resolution and relative ease and flexibility of application, EEG is optimally suited to investigate the temporal characteristics of the immediate brain response to online TUS as well as modulatory TUS effects on concurrent (online) or subsequent (offline) task-evoked or ongoing oscillatory activity. To allow measurement of a direct TUS-evoked EEG response, the TUS effect needs to be suprathreshold, as it is the case for TMS-evoked potentials

(TEPs). Lee and colleagues have indeed reported ultrasound-evoked potentials (UEPs) for TUS of the human visual (Lee et al., 2016b) and somatosensory cortex (Lee et al., 2015). In contrast, Legon and colleagues produced subthreshold modulations of the well-established somatosensory evoked potential (SEP) using online TUS of the primary somatosensory cortex (Legon et al., 2014) as well as the thalamus (Legon et al., 2018a). In the same way, SEPs, or event related potentials in general, can be used to assess the after-effects of offline TUS protocols on the respective neural (and associated cognitive) processes reflected by these time-locked EEG components. Beside evoked (i.e., phase-locked) potentials, induced (non-phase-locked) oscillatory de-/synchronization responses as well as spectral changes in the spontaneous resting-state EEG can be analyzed during (online) and after (offline) TUS.

Given that EEG requires the synchronization of large neuron populations to be picked up at the scalp level, and is particularly sensitive to neocortical (as compared to deep brain) and radial (as opposed to tangential) sources, some TUS-related neural effects will be missed by this technique. The particular strength of TUS, its high spatial precision and penetration depth, may at the same time limit the possibility of measuring its neural effects with EEG. The situation may be different when targeting small subcortical nuclei such as the thalamus, which have pronounced effects on oscillatory activity in larger neocortical areas. Another challenge may lie in the yet unclear temporal specificity of TUS. Based on the observation in rodents, that motor responses to TUS only occur after a certain (varying) delay, with TUS intensity modulating the response likelihood rather than the response magnitude (King et al., 2013), it is unclear how UEPs can be evoked without such latency jitter and how they can survive time-locked averaging. Future studies need to use high-density EEG (64-channels and more) to better localize such UEPs anatomically, ensuring they are not related to the auditory and somatosensory confounds associated with TUS application. However, if robust UEPs can be evoked, they may represent confounds when trying to modulate sensory evoked potentials, and their separate recording and subtraction would be required.

While TUS-related peripheral co-stimulation effects do exist (cf. section 8 for details), its auditory and somatosensory confounds can be considered minimal compared to the TMS “click” and the strong cutaneous sensations often associated with TMS and tES, respectively. Accordingly, the peripherally evoked potentials (PEPs) are not as pronounced in the EEG either and can be attenuated and masked more effectively. However, an artifact at the PRF may be visible in the EEG even when no buzzing sound is perceived by the subject, suggesting a technical origin. Luckily, most PRFs are outside the frequency range of interest for EEG studies, and can be easily removed with a respective low-pass filter. A major limitation for concurrent TUS-EEG comes from the requirement of acoustic coupling of the transducer to the scalp using gel. Therefore, no EEG electrodes can be mounted directly below the transducer, which limits the ability to measure radial sources for cortical TUS that are located directly below the transducer. However, for superficial tangential sources, such as the N20 component of the somatosensory evoked potential, originating in the posterior wall of the central sulcus, bipolar montages with electrodes located on both sides of the transducer can even be considered optimal (Legon et al., 2014). Beside the electrodes and cables, the textile fabric of the EEG cap would also prevent acoustic coupling, and either individual electrodes or EEG-caps with customized holes for the transducer are required.

Yet, transducer and electrode gels need to be sufficiently separated to avoid short circuits between EEG electrodes.

11.5. TMS

TMS-EMG of the primary motor cortex and measurement of motor evoked potentials (MEP) from the contralateral muscles, and possibly also combined TMS-EEG, can provide a readout of both online (Legon et al., 2018b; Fomenko et al., 2020) and offline TUS effects. TMS may be used to leverage its high temporal resolution, to distinguish between excitatory and inhibitory contributions, or to probe the system and quantify sub-threshold changes ("perturb-and-measure approach") that cannot be detected using EEG, MRI, or EMG alone. Additionally, since single- and paired-pulse TMS are widely used for measuring offline effects of TMS and tES (Rossini et al., 2015), this approach will also allow the comparison of offline TUS with established electromagnetic NIBS techniques. Moving forward, offline TMS protocols such as theta burst stimulation may be adapted to TUS. The frequencies used in these protocols likely interact with the dynamics of cellular processes like calcium influx (Huang et al., 2011), and hypothetically incorporating similar frequencies in TUS protocols could drive neuroplastic processes as well, with the caveat that TMS and TUS likely interact with different cellular processes or the same processes in different ways.

TMS and TUS have different spatial resolutions, which are, however, difficult to compare directly. Simulations using a variety of TMS coils have shown that even with very focal coils, the induced electric field (E-field) exceeds 50% of the maximum value in a volume spanning over 5 cm^3, and focality comes at the expense of depth, with a maximum achievable depth of less than 4 cm when keeping intensities within safety limits at the cortical surface (Thielscher and Kammer, 2004; Deng et al., 2013). In contrast, for 270, 500 and 650 kHz ultrasound transducers, the focal volumes (-3dB, i.e., approximately 50% of maximum intensity) are close to 0.4, 0.2 and 0.1 cm^3 respectively (Albelda Gimeno et al., 2019; Legon et al., 2014; Kim et al., 2014a), and focality can be further increased by using multi-element arrays (Darrow, 2019). The example focal sizes reported here rely on simulations in a spherical head model for TMS and measurements in free water for TUS, and actual focal size and shape within the brain will vary based on individual anatomy for both techniques, mainly depending on the skull for TUS (cf. section 2) but on the cortical gyrification for TMS. However, these examples illustrate that the TMS 'focus' spans an area on the order of centimetres, while the TUS focus spans an area on the order of millimetres. Note that both these foci are defined based on a ~50% decay from the maximal value at their center, irrespective of absolute stimulation intensity and thus the spatial extent of a neurophysiologically effective field strength. Additionally, the TMS induced E-field is stronger in the gyral crown compared to the sulcal wall, particularly when oriented perpendicular to the grey matter (GM) surface (Thielscher et al., 2011). Hypothetically, based on the cigar shaped ultrasound focus, greater interactions with GM could be achieved by aligning the focus along the sulcal wall. Finally, in addition to spatial extent and location, the orientation of neural structures relative to the direction of the E-field (Radman et al., 2009; Aberra et al., 2020) or ultrasound wave travel may influence both the effectiveness and type of neurons stimulated. Despite these differences, TMS can be used to

quantify TUS effect, as there remains sufficient overlap of the less focal E-field with the more focal acoustic field, and both TMS and TUS also cause trans-synaptic network effects beyond the neurons directly stimulated. However, when interpreting combined TUS-TMS-EMG findings one should keep in mind that even with the same intended anatomical target, the two techniques may stimulate different parts of the same area and/ or different types of neurons. Theoretically, such differences between the techniques may even form the basis for combining them to achieve specific or enhanced offline effects. Lastly, while neither single and paired pulse TMS nor online TUS are expected to produce any long-lasting after-effects, it cannot be ruled out entirely that unforeseen interactions between online TUS and TMS may lead to cumulative offline effects over the course of an experiment.

When targeting the same area, the ultrasound transducer, which must be acoustically coupled to the scalp, is placed between the TMS coil and the participant's head, and higher TMS intensities are required to account for the increased coil-to-cortex distance. Consequently, the transducer height is a limiting factor and some transducers and set-ups, e.g., those that require coupling-cones to achieve adequate positioning of the ultrasound focus, may not be suitable for combined TUS-TMS. Data available so far suggest that electromagnetic interactions between the coil and transducer do not significantly alter either the magnetic field or transducer output, except for a TMS pulse artefact in the ultrasound waveform, lasting less than 0.2 ms ((Legon et al., 2018b), unpublished data from Chen lab). However, since these interactions depend on factors such as the geometric design and insulation of each coil and transducer, this compatibility cannot be easily generalized and need to be established empirically for each device combination. Depending on the study goals, the transducer and coil may be attached to each other and neuronavigated as a single unit (Legon et al., 2018b; Fomenko et al., 2020), or positioned and navigated separately. Besides maintaining target accuracy, fixation methods (manual positioning, straps, mechanical arms, or robots) used to position coil and transducer relative to the head must account for head movements and ensure that the transducer remains acoustically coupled to the head.

12. Safety Considerations for TUS Exposure

Low-intensity transcranial ultrasound fundamentally relies on the transient deposition of acoustic energy onto brain tissue. The biophysical effects of ultrasound on brain tissue involve the complex propagation of acoustic energy through heterogenous intervening tissues and can lead to thermal and nonthermal (mechanical) bioeffects (cf. section 7), depending on the selected sonication regime (Fomenko et al., 2018; Legon et al., 2020; Pasquinelli et al., 2019). When designing TUS neuromodulation experiments on human participants, the selection of sonication parameters and manner of delivery and targeting of stimulation must be carefully considered to avoid injury and minimize discomfort to the participant.

As a relatively novel brain stimulation technique, TUS lacks definitive guidelines for safe energy deposition to the brain as of the time of this writing. Nevertheless, the United States Food and Drug Administration (FDA) provides intensity limits for diagnostic ultrasound, developed for obstetric and adult cephalic applications (Anon, 2017). Derated exposure limits for all tissues are

spatial peak pulse average (I_{SPPA}) < 190 W/cm^2, spatial peak temporal average (I_{SPTA}) < 720 mW/cm^2 and mechanical index (MI) < 1.9 (MI = peak negative pressure divided by the square root of the center frequency). Estimates of in-situ exposure are generally performed by hydrophone characterization of the transducer followed by derating by a set value of 0.3 dB/cm/MHz or by simulated estimated losses based on images of the skull. After derating, in situ estimates of ultrasound exposure in human TUS experiments have ranged as follows: $I_{SPPA:}$ = 1.1-14.39 W/cm^2; $I_{SPTA:}$ 0.067-5.8 W/cm^2; MI = 0.19-0.62 (Fomenko et al., 2018; Lee et al., 2020; Legon et al., 2020). In general, the I_{SPTA} is related to thermal effects, while I_{SPPA} and MI are related to the potential for cavitation in the sonicated tissues (Fomenko et al., 2018). It should be noted that while in some of the above mentioned studies, I_{SPTA} values were above the stated regulatory guidelines for diagnostic imaging, the resulting thermal increase in brain temperature (which has to be calculated for such cases according to FDA guidelines) was typically well below 1°C (e.g., Lee et al., 2016a), which can be considered safe for brain tissue.

Obtaining biopsies or tissue samples is far more tractable in animal models than humans, making them an excellent tool for safety studies. Histologic analysis of brain tissue can reveal subtle inflammatory changes that may not manifest externally in the behavior or outward appearance of the organism. Small animal (Kamimura et al., 2016), large animal (Lee et al., 2016c; Dallapiazza et al., 2017; Yoon et al., 2019; Verhagen et al., 2019; Gaur et al., 2020), and limited human (Stern et al., 2021) studies have been conducted to assess the histological appearance of brain tissue sonicated with low-intensity TUS. In these kinds of experiments, the brain is fixed and extracted following sonication and typically stained with hematoxylin and eosin, and occasionally TUNEL for indications of morphological changes, cell damage, and apoptosis (Mehić et al., 2014; Gaur et al., 2020). To date, although the majority of studies have found no indications of cell damage, one sheep study reported the presence of microhemorrhages after repeated sonication of the visual cortex at a relatively high in-situ I_{SPPA} of 10.5 W/cm^2 (Lee et al., 2016c). Sheep were chosen due to the structural similarities between the sheep and human craniums (thickness, radius of curvature, and porosity) and the non-homogeneous and gyrencephalic neuroanatomical structures. This study unfortunately lacked a negative control for comparison (Lee et al., 2016c). No edema, necrosis, or local inflammatory responses were found, likely implicating post-mortem brain extraction rather than sonication as the cause. Notably, a follow-up study in sheep using higher pressure intensities and more sonications than the Lee study also found no inflammatory markers in sonicated brains. The finding of microhemorrhages in both unsonicated and sonicated animals, as well as bone fragments from the extraction process, and the lack of inflammatory markers suggests hemorrhages were not from the ultrasound (Gaur et al., 2020).

To date, only a single human report has examined the histological appearance of sonicated brain tissue, specifically temporal lobe specimens from resected epileptogenic zones (Stern et al., 2021). After sonication through the temporal bone at in situ time-averaged intensities of 0.72-5.76 W/cm^2, histological examination of the sonicated neural tissue showed acidophilic neurons and extravasation in one patient out of eight. However, due to similar changes being observed in the non-sonicated control samples, the findings were suggestive that it was not a TUS-related effect (Stern et al., 2021).

To date, no "serious adverse events" have been causally attributed to low-intensity TUS, and even the occurrence of "mild/moderate adverse events", such as headache, could not be unambiguously attributed to the application of TUS (see below). However, a number of common "non-adverse" and transient side effects such as tingling, warming, and a high-pitched noise have been described in several studies (Fomenko et al., 2020; Legon et al., 2020), and are mainly limited to the duration of sonication and to the scalp transducer placement site. A recent retrospective human study specifically addressed perceived tolerance to participation in low-intensity TUS experiments and potential contribution of the ultrasound intervention to reported symptoms (Legon et al., 2020). A group of 64 participants from several TUS neuromodulation studies at a single site completed a questionnaire at timepoints ranging from immediately post-experiment to 22 months afterwards. Results showed that 7/64 participants reported mild/moderate symptoms including neck pain, difficulty paying attention, muscles twitches and anxiety which they felt were possibly or probably related to ultrasound application. No symptoms were attributed by the subjects to have a definitive causal link to ultrasound exposure. Interestingly, for the estimated acoustic intensities used in this report (I_{SPPA}= 11.56 - 17.12 W/cm^2), the authors found a positive linear correlation between positive symptom report and increasing intensity (Legon et al., 2020). A limitation of this report, however, was that other non-invasive brain stimulation and acquisition techniques such as TMS, EEG, EMG, and MRI were used during these experiments (Legon et al., 2020). Given that short-term and nonspecific symptoms such as anxiety and noise-induced headache have been reported in both neuroimaging (Cosottini et al., 2014) and transcranial magnetic stimulation (Ferrulli et al., 2021) experiments, definite attribution of these symptoms to TUS was not possible.

The neuromodulatory effects of low-intensity TUS on human neural activity have demonstrated robust and reproducible suppressive (Legon et al., 2018b, 2018a; Fomenko et al., 2020) and excitatory (Lee et al., 2015, 2016b; Gibson et al., 2018; Schimek et al., 2020; Yu et al., 2020) effects. To date, these effects have been transient and reversible, supporting the safety profile of current sonication regimes (Lee et al., 2020; Legon et al., 2020). Nevertheless, with reports of other non-invasive brain stimulation modalities such as TMS (Lenoir et al., 2018; Udupa et al., 2020) and transcranial direct current stimulation (Ekici, 2015) eliciting unexpected seizure activity in human subjects (but see Rossi et al., (2021) for a comprehensive discussion), a careful assessment of participant demographics might be prudent when designing TUS experiments. On the other hand, rodent and non-human primate studies have shown that certain TUS parameters suppress seizure activity in acute epilepsy models (Hakimova et al., 2015; Zou et al., 2020), highlighting the importance of parameter selection, and future research into TUS mechanisms of actions on hyperexcitable neural networks and circuits.

Overall, the current literature supports low-intensity TUS as a safe non-invasive brain stimulation technique, with an adverse event profile similar or milder than that established for NIBS techniques such as TMS and tES. Reports of transient, reversible, and tolerable short-term side effects are typically isolated to the stimulation itself and are similar to those of TMS experiments, and transient adverse events, such as headaches, are comparable to TMS.

13. Conclusions and future perspectives

TUS is a promising non-invasive technique with greater depth penetration and higher spatial resolution compared to current NIBS methods. The studies summarized here showed that TUS has the potential to advance neuroscience research and to be developed as a novel non-invasive treatment for neurological and psychiatric disorders. Further animal and human studies are needed to provide better understanding of the mechanisms of action of TUS, establish its safety limits in humans, develop effective protocols to induce brain plasticity, and define the optimal TUS parameters for each disorder and targeted brain region. Pilot studies followed by well-designed randomized controlled trials will be also needed to establish the role to TUS in the treatment of brain disorders.

Acknowledgements

G.D. was supported by a German Research foundation research fellowship (DFG DA 2374/1-1) and Krembil Post-Doctoral Fellowship Award. E.F. was supported by a UKRI FLF - Medical Research Council (grants MR/T023007/1). A.F. was supported by the CIHR Banting and Best Doctoral Award and the University of Manitoba Clinician Investigator Program. K.R.M. was supported by the Ruth L. Kirschstein Postdoctoral Individual National Research Service Award (1F32HL149458-01A1). T.N. was supported by a grant from the Boehringer Ingelheim Foundation (BIS) to T.O.B.

Conflicts of interest

None declared.

References

Abe J, Okazawa M, Adachi R, Matsumura K, Kobayashi S. Primary cold-sensitive neurons in acutely dissociated cells of rat hypothalamus. Neurosci Lett 2003;342:29–32. https://doi.org/10.1016/s0304-3940(03)00239-8.

Aberra AS, Wang B, Grill WM, Peterchev AV. Simulation of transcranial magnetic stimulation in head model with morphologically-realistic cortical neurons. Brain Stimul 2020;13:175–89. https://doi.org/10.1016/j.brs.2019.10.002.

Ai L, Bansal P, Mueller J, Legon W. Effects of transcranial focused ultrasound on human primary motor cortex using 7T fMRI: a pilot study. BMC Neurosci 2018;19:56. https://doi.org/10.1186/s12868-018-0456-6.

Ai L, Mueller J, Grant A, Eryaman Y, Wynn Legon null. Transcranial focused ultrasound for BOLD fMRI signal modulation in humans. Annu Int Conf IEEE Eng Med Biol Soc 2016;2016:1758–61. https://doi.org/10.1109/EMBC.2016.7591057.

Albelda Gimeno L, Martin E, Wright O, Treeby B. Experimental assessment of skull aberration and transmission loss at 270 kHz for focused ultrasound stimulation of the primary visual cortex. IEEE Int Ultrasonics Symposiums (IUS) 2019:556–9. https://doi.org/10.1109/ULTSYM.2019.8926097.

Anon. Marketing Clearance of Diagnostic Ultrasound Systems and Transducers: Draft Guidance for Industry and Food and Drug Administration Staff. 2017.

Auboiroux V, Viallon M, Roland J, Hyacinthe J-N, Petrusca L, Morel DR, et al. ARFI-prepared MRgHIFU in liver: simultaneous mapping of ARFI-displacement and temperature elevation, using a fast GRE-EPI sequence. Magn Reson Med 2012;68:932–46. https://doi.org/10.1002/mrm.23309.

Aubry JF, Tanter M, Pernot M, Thomas J-L, Fink M. Experimental demonstration of noninvasive transskull adaptive focusing based on prior computed tomography scans. J Acoust Soc Am 2003;113:84–93. https://doi.org/10.1121/1.1529663.

Bachtiar V, Near J, Johansen-Berg H, Stagg CJ. Modulation of GABA and resting state functional connectivity by transcranial direct current stimulation. Elife 2015;4:e08789. https://doi.org/10.7554/eLife.08789.

Bachtold MR, Rinaldi PC, Jones JP, Reines F, Price LR. Focused ultrasound modifications of neural circuit activity in a mammalian brain. Ultrasound Med Biol 1998;24:557–65. https://doi.org/10.1016/s0301-5629(98)00014-3.

Badran BW, Caulfield KA, Stomberg-Firestein S, Summers PM, Dowdle LT, Savoca M, et al. Sonication of the anterior thalamus with MRI-Guided transcranial focused ultrasound (tFUS) alters pain thresholds in healthy adults: A double-blind, sham-controlled study. Brain Stimul 2020;13:1805–12. https://doi.org/10.1016/j.brs.2020.10.007.

Baek H, Sariev A, Dong S, Royer S, Kim H. Cerebellar low-intensity focused ultrasound stimulation can normalize asymmetrical hemispheric delta power after mouse ischemic stroke. Brain Stimul 2019;12:487. https://doi.org/10.1016/j.brs.2018.12.591.

Barnett SB, Rott HD, ter Haar GR, Ziskin MC, Maeda K. The sensitivity of biological tissue to ultrasound. Ultrasound Med Biol 1997;23:805–12. https://doi.org/10.1016/s0301-5629(97)00027-6.

Beisteiner R, Matt E, Fan C, Baldysiak H, Schönfeld M, Philippi Novak T, et al. Transcranial Pulse Stimulation with Ultrasound in Alzheimer's Disease-A New Navigated Focal Brain Therapy. Adv Sci 2020;7:1902583. https://doi.org/10.1002/advs.201902583.

Bergmann TO. Brain State-Dependent Brain Stimulation. Front Psychol 2018;9:2108. https://doi.org/10.3389/fpsyg.2018.02108.

Bergmann TO, Hartwigsen G. Inferring Causality from Noninvasive Brain Stimulation in Cognitive Neuroscience. J Cogn Neurosci 2021;33:195–225. https://doi.org/10.1162/jocn_a_01591.

Bergmann TO, Karabanov A, Hartwigsen G, Thielscher A, Siebner HR. Combining non-invasive transcranial brain stimulation with neuroimaging and electrophysiology: Current approaches and future perspectives. Neuroimage 2016;140:4-19. https://doi.org/10.1016/j.neuroimage.2016.02.012.

Bergmann TO, Varatheeswaran R, Hanlon CA, Madsen KH, Thielscher A, Siebner HR. Concurrent TMS-fMRI for causal network perturbation and proof of target engagement. Neuroimage 2021;237:118093. https://doi.org/10.1016/j.neuroimage.2021.118093.

Bian T, Meng W, Qiu M, Zhong Z, Lin Z, Zou J, et al. Noninvasive Ultrasound Stimulation of Ventral Tegmental Area Induces Reanimation from General Anaesthesia in Mice. Research 2021;2021:2674692. https://doi.org/10.34133/2021/2674692.

Blackmore DG, Turpin F, Palliyaguru T, Evans HT, Chicoteau A, Lee W, et al. Low-intensity ultrasound restores long-term potentiation and memory in senescent mice through pleiotropic mechanisms including NMDAR signaling. Mol Psychiatry 2021, https://doi.org/doi:10.1038/s41380-021-01129-7.

Bongioanni A, Folloni D, Verhagen L, Sallet J, Klein-Flügge MC, Rushworth MFS. Activation and disruption of a neural mechanism for novel choice in monkeys. Nature 2021;591:270–4. https://doi.org/10.1038/s41586-020-03115-5.

Bossy E, Laugier P, Peyrin F, Padilla F. Attenuation in trabecular bone: A comparison between numerical simulation and experimental results in human femur. J Acoust Soc Am 2007;122:2469–75. https://doi.org/10.1121/1.2766779.

Boulant JA. The effect of firing rate on preoptic neuronal thermosensitivity. J Physiol 1974;240:661–9. https://doi.org/10.1113/jphysiol.1974.sp010628.

Braun V, Blackmore J, Cleveland RO, Butler CR. Transcranial ultrasound stimulation in humans is associated with an auditory confound that can be effectively masked. Brain Stimul 2020;13:1527–1534. https://doi.org/10.1016/j.brs.2020.08.014.

Brennen CE. Cavitation and Bubble Dynamics. Cambridge: Cambridge University Press; 2013. https://doi.org/10.1017/CBO9781107338760.

Brodt S, Gais S, Beck J, Erb M, Scheffler K, Schonauer M. Fast track to the neocortex: A memory engram in the posterior parietal cortex. Science 2018;362:1045-1048. https://doi.org/10.1126/science.aau2528.

Cain JA., Spivak NM, Coetzee JP, Crone JS, Johnson MA, Lutkenhoff ES, et al. Ultrasonic Thalamic Stimulation in Chronic Disorders of Consciousness. Brain Stimul 2021;0. https://doi.org/10.1016/j.brs.2021.01.008.

Cain JA., Visagan S, Johnson MA, Crone J, Blades R, Spivak NM, et al. Real time and delayed effects of subcortical low intensity focused ultrasound. Sci Rep 2021;11:6100. https://doi.org/10.1038/s41598-021-85504-y.

Caro AC, Hankenson FC, Marx JO. Comparison of thermoregulatory devices used during anesthesia of C57BL/6 mice and correlations between body temperature and physiologic parameters. J Am Assoc Lab Anim Sci 2013;52:577–83.

Castro-Alamancos MA, Donoghue JP, Connors BW. Different forms of synaptic plasticity in somatosensory and motor areas of the neocortex. J Neurosci 1995;15:5324–33. https://doi.org/10.1523/JNEUROSCI.15-07-05324.1995.

Chaplin V, Phipps MA, Caskey CF. A random phased-array for MR-guided transcranial ultrasound neuromodulation in non-human primates. Phys Med Biol 2018;63:105016. https://doi.org/10.1088/1361-6560/aabeff.

Chaplin V, Phipps MA, Jonathan SV, Grissom WA, Yang PF, Chen LM, et al. On the accuracy of optically tracked transducers for image-guided transcranial ultrasound. Int J Comput Assist Radiol Surg 2019;14:1317–27. https://doi.org/10.1007/s11548-019-01988-0.

Chen J, Watkins R, Pauly KB. Optimization of encoding gradients for MR-ARFI. Magn Reson Med 2010;63:1050–8. https://doi.org/10.1002/mrm.22299.

Chen R, Classen J, Gerloff C, Celnik P, Wassermann EM, Hallett M, et al. Depression of motor cortex excitability by low-frequency transcranial magnetic stimulation. Neurology 1997, 48:1398–1403. https://doi.org/10.1212/wnl.48.5.1398.

Churchland MM, Yu BM, Cunningham JP, Sugrue LP, Cohen MR, Corrado GS, et al. Stimulus onset quenches neural variability: a widespread cortical phenomenon. Nat Neurosci 2010;13:369–78. https://doi.org/10.1038/nn.2501.

Cincotta M, Giovannelli F, Borgheresi A, Balestrieri F, Toscani L, Zaccara G, Carducci F, Viggiano MP, Rossi S. Optically tracked neuronavigation increases the stability of hand-held focal coil positioning: Evidence from “transcranial” magnetic stimulation-induced electrical field measurements. Brain Stimul 2010;3:119–123. https://doi.org/10.1016/j.brs.2010.01.001.

Citri A, Malenka RC: Synaptic plasticity: multiple forms, functions, and mechanisms. Neuropsychopharmacology 2008, 33:18–41. https://doi.org/10.1038/sj.npp.1301559.

Clement GT, Hynynen K. Correlation of ultrasound phase with physical skull properties. Ultrasound Med Biol 2002a;28:617–24. https://doi.org/10.1016/s0301-5629(02)00503-3.

Clement GT, Hynynen K. A non-invasive method for focusing ultrasound through the human skull. Phys Med Biol 2002b;47:1219–36. https://doi.org/10.1088/0031-9155/47/8/301.

Clement GT., White J, Hynynen K. Investigation of a large-area phased array for focused ultrasound surgery through the skull. Phys Med Biol 2000;45(4):1071-83. https://doi.org/10.1088/0031-9155/45/4/319.

Clennell B, Steward TGJ, Elley M, Shin E, Weston M, Drinkwater BW, et al. Transient ultrasound stimulation has lasting effects on neuronal excitability. Brain Stimul 2021;0. https://doi.org/10.1016/j.brs.2021.01.003.

Cosottini M, Frosini D, Biagi L, Pesaresi I, Costagli M, Tiberi G, et al. Short-term side-effects of brain MR examination at 7 T: a single-centre experience. Eur Radiol 2014;24:1923–8. https://doi.org/10.1007/s00330-014-3177-y.

Coste B, Mathur J, Schmidt M, Earley TJ, Ranade S, Petrus MJ, et al. Piezo1 and Piezo2 are essential components of distinct mechanically activated cation channels. Science 2010;330:55–60. https://doi.org/10.1126/science.1193270.

Cuypers K, Marsman A. Transcranial magnetic stimulation and magnetic resonance spectroscopy: Opportunities for a bimodal approach in human neuroscience. Neuroimage 2021;224:117394. https://doi.org/10.1016/j.neuroimage.2020.117394.

Dalecki D. Mechanical bioeffects of ultrasound. Annu Rev Biomed Eng 2004;6:229–48. https://doi.org/10.1146/annurev.bioeng.6.040803.140126.

Dallapiazza RF, Timbie KF, Holmberg S, Gatesman J, Lopes MB, Price RJ, et al. Noninvasive neuromodulation and thalamic mapping with low-intensity focused ultrasound. Journal of Neurosurgery 2017;128:875–84. https://doi.org/10.3171/2016.11.JNS16976.

Darrow DP. Focused Ultrasound for Neuromodulation. Neurotherapeutics 2019;16:88–99. https://doi.org/10.1007/s13311-018-00691-3.

Darrow DP, O'Brien P, Richner TJ, Netoff TI, Ebbini ES. Reversible neuroinhibition by focused ultrasound is mediated by a thermal mechanism. Brain Stimul 2019;12:1439–47. https://doi.org/10.1016/j.brs.2019.07.015.

Deffieux T, Demene C, Pernot M, Tanter M. Functional ultrasound neuroimaging: a review of the preclinical and clinical state of the art. Curr Opin Neurobiol 2018;50:128–35. https://doi.org/10.1016/j.conb.2018.02.001.

Deffieux T, Konofagou EE. Numerical study of a simple transcranial focused ultrasound system applied to blood-brain barrier opening. IEEE Trans Ultrason Ferroelectr Freq Control 2010;57:2637–53. https://doi.org/10.1109/TUFFC.2010.1738.

Deffieux T, Younan Y, Wattiez N, Tanter M, Pouget P, Aubry J-F Low-Intensity Focused Ultrasound Modulates Monkey Visuomotor Behavior. Current Biology 23:2430–2433. https://doi.org/10.1016/j.cub.2013.10.029.

Deng ZD, Lisanby SH, Peterchev AV. Electric field depth-focality tradeoff in transcranial magnetic stimulation: simulation comparison of 50 coil designs. Brain Stimul 2013;6:1–13. https://doi.org/10.1016/j.brs.2012.02.005.

D'Souza M, Chen KS, Rosenberg J, Elias WJ, Eisenberg HM, Gwinn R, et al. Impact of skull density ratio on efficacy and safety of magnetic resonance-guided focused ultrasound treatment of essential tremor. J Neurosurg 2019;132:1392–7. https://doi.org/10.3171/2019.2.JNS183517.

Eguchi K, Shindo T, Ito K, Ogata T, Kurosawa R, Kagaya Y, et al. Whole-brain low-intensity pulsed ultrasound therapy markedly improves cognitive dysfunctions in mouse models of dementia - Crucial roles of endothelial nitric oxide synthase. Brain Stimul 2018;11:959–73. https://doi.org/10.1016/j.brs.2018.05.012.

Ekici B. Transcranial direct current stimulation-induced seizure: analysis of a case. Clin EEG Neurosci 2015;46:169. https://doi.org/10.1177/1550059414540647.

Elias WJ, Huss D, Voss T, Loomba J, Khaled M, Zadicario E, et al. A Pilot Study of Focused Ultrasound Thalamotomy for Essential Tremor. N Engl J Med 2013;369:640–8. https://doi.org/10.1056/NEJMoa1300962.

Ferrulli A, Massarini S, Macrì C, Luzi L. Safety and tolerability of repeated sessions of deep transcranial magnetic stimulation in obesity. Endocrine 2021;71:331–43. https://doi.org/10.1007/s12020-020-02496-x.

Fitzpatrick JM, West JB, Maurer CR. Predicting error in rigid-body point-based registration. IEEE Trans Med imaging 1998;17:694–702. https://doi.org/10.1109/42.736021.

Folloni D, Verhagen L, Mars RB, Fouragnan E, Constans C, Aubry J-F, et al. Manipulation of Subcortical and Deep Cortical Activity in the Primate Brain Using Transcranial Focused Ultrasound Stimulation. Neuron 2019;101:1109-1116.e5. https://doi.org/10.1016/j.neuron.2019.01.019.

Fomenko A, Chen K-HS, Nankoo J-F, Saravanamuttu J, Wang Y, El-Baba M, et al. Systematic examination of low-intensity ultrasound parameters on human motor cortex excitability and behavior. ELife 2020;9:e54497. https://doi.org/10.7554/eLife.54497.

Fomenko A, Neudorfer C, Dallapiazza RF, Kalia SK, Lozano AM. Low-intensity ultrasound neuromodulation: An overview of mechanisms and emerging human applications. Brain Stimul 2018;11:1209–17. https://doi.org/10.1016/j.brs.2018.08.013.

Foster KR, Wiederhold ML. Auditory responses in cats produced by pulsed ultrasound. J Acoust Soc Am 1978;63:1199–1205. https://doi.org/10.1121/1.381829.

Fouragnan EF, Chau BKH, Folloni D, Kolling N, Verhagen L, Klein-Flügge M, et al. The macaque anterior cingulate cortex translates counterfactual choice value into actual behavioral change. Nat Neurosci 2019;22:797–808. https://doi.org/10.1038/s41593-019-0375-6.

Frey AH. Auditory system response to radio frequency energy. Technical note. Aerosp Med 1961;32:1140–1142.

Fry FJ, Ades HW, Fry WJ. Production of reversible changes in the central nervous system by ultrasound. Science 1958;127:83–4. https://doi.org/10.1126/science.127.3289.83.

Fry WJ, Tucker D, Fry FJ, Wulff VJ. Physical Factors Involved in Ultrasonically Induced Changes in Living Systems: II. Amplitude Duration Relations and the Effect of Hydrostatic Pressure for Nerve Tissue. J Acoust Soc Am 1951;23:364–8. https://doi.org/10.1121/1.1906774.

FUS-Foundation Focused Ultrasound for Glioblastoma Workshop Summary. Charlottesville, VA. 2015.

Gaur P, Casey KM, Kubanek J, Li N, Mohammadjavadi M, Saenz Y, et al. Histologic safety of transcranial focused ultrasound neuromodulation and magnetic resonance acoustic radiation force imaging in rhesus macaques and sheep. Brain Stimul 2020;13:804–14. https://doi.org/10.1016/j.brs.2020.02.017.

Gavrilov LR, Tsirulnikov EM, Davies I ab I. Application of focused ultrasound for the stimulation of neural structures. Ultrasound Med Biol 1996;22:179–92. https://doi.org/10.1016/0301-5629(96)83782-3.

Gibson BC, Sanguinetti JL, Badran BW, Yu AB, Klein EP, Abbott CC, et al. Increased Excitability Induced in the Primary Motor Cortex by Transcranial Ultrasound Stimulation. Front Neurol 2018;9. https://doi.org/10.3389/fneur.2018.01007.

Guerra A, Vicenzini E, Cioffi E, Colella D, Cannavacciuolo A, Pozzi S, et al. Effects of Transcranial Ultrasound Stimulation on Trigeminal Blink Reflex Excitability. Brain Sci 2021;11:645. https://doi.org/10.3390/brainsci11050645.

Guo H, Hamilton M, Offutt SJ, Gloeckner CD, Li T, Kim Y, et al. Ultrasound Produces Extensive Brain Activation via a Cochlear Pathway. Neuron 2018;98:1020-1030.e4. https://doi.org/10.1016/j.neuron.2018.04.036.

Guo S, Zhuo J, Li G, Gandhi D, Dayan M, Fishman P, et al. Feasibility of ultrashort echo time images using full-wave acoustic and thermal modeling for transcranial MRI-guided focused ultrasound (tcMRgFUS) planning. Phys Med Biol 2019;64:095008. https://doi.org/10.1088/1361-6560/ab12f7.

Hakimova H, Kim S, Chu K, Lee SK, Jeong B, Jeon D. Ultrasound stimulation inhibits recurrent seizures and improves behavioral outcome in an experimental model of mesial temporal lobe epilepsy. Epilepsy Behav 2015;49:26–32. https://doi.org/10.1016/j.yebeh.2015.04.008.

Hameroff S, Trakas M, Duffield C, Annabi E, Gerace MB, Boyle P, et al. Transcranial Ultrasound (TUS) Effects on Mental States: A Pilot Study. Brain Stimul 2013;6:409–15. https://doi.org/10.1016/j.brs.2012.05.002.

Harvey EN. The effect of high frequency sound waves on heart muscle and other irritable tissues. Am J Physiol 1929;91:284–90. https://doi.org/10.1152/ajplegacy.1929.91.1.284.

Herwig U, Schönfeldt-Lecuona C, Wunderlich AP, von Tiesenhausen C, Thielscher A, Walter H, et al. The navigation of transcranial magnetic stimulation. Psychiatry Res 2001;108:123–31. https://doi.org/10.1016/s0925-4927(01)00121-4.

Hofstetter S, Friedmann N, Assaf Y. Rapid language-related plasticity: microstructural changes in the cortex after a short session of new word learning. Brain Struct Funct 2017;222:1231–41. https://doi.org/10.1007/s00429-016-1273-2.

Huang SL, Chang CW, Lee YH, Yang FY. Protective Effect of Low-Intensity Pulsed Ultrasound on Memory Impairment and Brain Damage in a Rat Model of Vascular Dementia. Radiology 2016;282:113–22. https://doi.org/10.1148/radiol.2016160095.

Huang YZ, Edwards MJ, Rounis E, Bhatia KP, Rothwell JC. Theta burst stimulation of the human motor cortex. Neuron 2005;45:201–6. https://doi.org/10.1016/j.neuron.2004.12.033.

Huang YZ, Rothwell JC, Chen RS, Lu CS, Chuang WL. The theoretical model of theta burst form of repetitive transcranial magnetic stimulation. Clin Neurophysiol 2011;122:1011–8. https://doi.org/10.1016/j.clinph.2010.08.016.

Ide M, Hidaka S. Tactile stimulation can suppress visual perception. Sci Rep 2013;3:3453. https://doi.org/10.1038/srep03453.

Jing Y, Meral FC, Clement GregT. Time-reversal transcranial ultrasound beam focusing using a k-space method. Phys Med Biol 2012;57:901–17. https://doi.org/10.1088/0031-9155/57/4/901.

Jung NY, Rachmilevitch I, Sibiger O, Amar T, Zadicario E, Chang JW. Factors Related to Successful Energy Transmission of Focused Ultrasound through a Skull : A Study in Human Cadavers and Its Comparison with Clinical Experiences. J Korean Neurosurg Soc 2019;62:712–22. https://doi.org/10.3340/jkns.2018.0226.

Kahneman D. Method, findings, and theory in studies of visual masking. Psychol Bull 1968;70:404–25. https://doi.org/10.1037/h0026731.

Kamimura HAS, Wang S, Chen H, Wang Q, Aurup C, Acosta C, et al. Focused ultrasound neuromodulation of cortical and subcortical brain structures using 1.9 MHz. Med Phys 2016;43:5730–5. https://doi.org/10.1118/1.4963208.

Kammer T. Phosphenes and transient scotomas induced by magnetic stimulation of the occipital lobe: their topographic relationship. Neuropsychologia 1999;37:191–8. https://doi.org/10.1016/s0028-3932(98)00093-1.

Kaye EA, Chen J, Pauly KB. Rapid MR-ARFI Method for Focal Spot Localization during Focused Ultrasound Therapy. Magn Reson Med 2011;65:738–43. https://doi.org/10.1002/mrm.22662.

Khalighinejad N, Bongioanni A, Verhagen L, Folloni D, Attali D, Aubry J-F, et al. A Basal Forebrain-Cingulate Circuit in Macaques Decides It Is Time to Act. Neuron 2020;105:370-384.e8. https://doi.org/10.1016/j.neuron.2019.10.030.

Kim H, Chiu A, Lee SD, Fischer K, Yoo SS. Focused ultrasound-mediated non-invasive brain stimulation: examination of sonication parameters. Brain Stimul 2014;7:748–56. https://doi.org/10.1016/j.brs.2014.06.011.

Kim H, Chiu A, Park S, Yoo SS. Image-guided Navigation of Single-element Focused Ultrasound Transducer. Int J Imaging Syst Technol 2012a;22:177–84. https://doi.org/10.1002/ima.22020.

Kim H, Park M-A, Wang S, Chiu A, Fischer K, Yoo SS. PET⁄CT imaging evidence of FUS-mediated (18)F-FDG uptake changes in rat brain. Med Phys 2013;40:033501. https://doi.org/10.1118/1.4789916.

Kim H, Taghados SJ, Fischer K, Maeng L-S, Park S, Yoo SS. Noninvasive transcranial stimulation of rat abducens nerve by focused ultrasound. Ultrasound Med Biol 2012b;38:1568–75. https://doi.org/10.1016/j.ultrasmedbio.2012.04.023.

Kim Y, Hall TL, Xu Z, Cain CA. Transcranial histotripsy therapy: a feasibility study. IEEE Trans Ultrason Ferroelectr Freq Control 2014;61:582–93. https://doi.org/10.1109/TUFFC.2014.2947.

King RL, Brown JR, Newsome WT, Pauly KB. Effective Parameters for Ultrasound-Induced In Vivo Neurostimulation. Ultrasound Med Biol 2013;39:312–31. https://doi.org/10.1016/j.ultrasmedbio.2012.09.009.

Kral F, Puschban EJ, Riechelmann H, Freysinger W. Comparison of optical and electromagnetic tracking for navigated lateral skull base surgery. Int J Med Robot 2013;9:247–52. https://doi.org/10.1002/rcs.1502.

Kubanek J, Brown J, Ye P, Pauly KB, Moore T, Newsome W. Remote, brain region–specific control of choice behavior with ultrasonic waves. Sci Adv 2020;6:eaaz4193. https://doi.org/10.1126/sciadv.aaz4193.

Kubanek J, Shi J, Marsh J, Chen D, Deng C, Cui J. Ultrasound modulates ion channel currents. Sci Rep 2016;6:24170. https://doi.org/10.1038/srep24170.

Kubanek J, Shukla P, Das A, Baccus SA, Goodman MB. Ultrasound Elicits Behavioral Responses through Mechanical Effects on Neurons and Ion Channels in a Simple Nervous System. J Neurosci 2018;38:3081–91. https://doi.org/10.1523/JNEUROSCI.1458-17.2018.

Kyriakou A, Neufeld E, Werner B, Paulides MM, Szekely G, Kuster N. A review of numerical and experimental compensation techniques for skull-induced phase aberrations in transcranial focused ultrasound. Int J Hyperthermia 2014;30:36–46. https://doi.org/10.3109/02656736.2013.861519.

Labadie RF, Davis BM, Fitzpatrick JM. Image-guided surgery: What is the accuracy? Curr Opin Otolaryngol Head Neck Surg 2005;13:27–31. https://doi.org/10.1097/00020840-200502000-00008.

Lee W, Chung YA, Jung Y, Song I-U, Yoo SS. Simultaneous acoustic stimulation of human primary and secondary somatosensory cortices using transcranial focused ultrasound. BMC Neurosci 2016a;17:68. https://doi.org/10.1186/s12868-016-0303-6.

Lee W, Croce P, Margolin RW, Cammalleri A, Yoon K, Yoo SS. Transcranial focused ultrasound stimulation of motor cortical areas in freely-moving awake rats. BMC Neurosci 2018;19:57. https://doi.org/10.1186/s12868-018-0459-3.

Lee W, Kim H, Jung Y, Song I-U, Chung YA, Yoo SS. Image-Guided Transcranial Focused Ultrasound Stimulates Human Primary Somatosensory Cortex. Sci Rep 2015;5:8743. https://doi.org/10.1038/srep08743.

Lee W, Kim H-C, Jung Y, Chung YA, Song I-U, Lee JH, et al. Transcranial focused ultrasound stimulation of human primary visual cortex. Sci Rep 2016b;6:34026. https://doi.org/10.1038/srep34026.

Lee W, Lee SD, Park MY, Foley L, Purcell-Estabrook E, Kim H, et al. Image-Guided Focused Ultrasound-Mediated Regional Brain Stimulation in Sheep. Ultrasound Med Biol 2016c;42:459–70. https://doi.org/10.1016/j.ultrasmedbio.2015.10.001.

Lee W, Weisholtz DS, Strangman GE, Yoo SS. Safety Review and Perspectives of Transcranial Focused Ultrasound Brain Stimulation. Brain Neurorehabi 2020;14. https://doi.org/10.12786/bn.2021.14.e4.

Lefaucheur JP, Aleman A, Baeken C, Benninger DH, Brunelin J, Di Lazzaro V, et al. Evidence-based guidelines on the therapeutic use of repetitive transcranial magnetic stimulation (rTMS): An update (2014–2018). Clin Neurophysiol 2020, 131:474–528. https://doi.org/10.1016/j.clinph.2019.11.002.

Legon W, Adams S, Bansal P, Patel PD, Hobbs L, Ai L, et al. A retrospective qualitative report of symptoms and safety from transcranial focused ultrasound for neuromodulation in humans. Sci Rep 2020;10:1–10. https://doi.org/10.1038/s41598-020-62265-8.

Legon W, Ai L, Bansal P, Mueller J. Neuromodulation with single-element transcranial focused ultrasound in human thalamus. Hum Brain Map 2018a;39:1995–2006. https://doi.org/10.1002/hbm.23981.

Legon W, Bansal P, Tyshynsky R, Ai L, Mueller J. Transcranial focused ultrasound neuromodulation of the human primary motor cortex. Sci Rep 2018b;8:10007. https://doi.org/10.1038/s41598-018-28320-1.

Legon W, Sato TF, Opitz A, Mueller J, Barbour A, Williams A, et al. Transcranial focused ultrasound modulates the activity of primary somatosensory cortex in humans. Nat Neurosci 2014;17:322–9. https://doi.org/10.1038/nn.3620.

Legrand M, Galineau L, Novell A, Planchez B, Brizard B, Leman S, et al. Efficacy of chronic ultrasound neurostimulation on behaviors and distributed brain metabolism in depressive-like mice. BioRxiv 2019:813006. https://doi.org/10.1101/813006.

Lele PP. Effects of focused ultrasonic radiation on peripheral nerve, with observations on local heating. Exp Neurol 1963;8:47–83. https://doi.org/10.1016/0014-4886(63)90008-6.

Lenoir C, Algoet M, Vanderclausen C, Peeters A, Santos SF, Mouraux A. Report of one confirmed generalized seizure and one suspected partial seizure induced by deep continuous theta burst stimulation of the right operculo-insular cortex. Brain Stimul 2018;11:1187–8. https://doi.org/10.1016/j.brs.2018.05.004.

Lin WT, Chen RC, Lu WW, Liu SH, Yang FY. Protective effects of low-intensity pulsed ultrasound on aluminum-induced cerebral damage in Alzheimer's disease rat model. Sci Rep 2015;5:9671. https://doi.org/10.1038/srep09671.

Liu C, Yu K, Niu X, He B. Transcranial Focused Ultrasound Enhances Sensory Discrimination Capability through Somatosensory Cortical Excitation. Ultrasound Med Biol 2021;47:1356–1366. https://doi.org/10.1016/j.ultrasmedbio.2021.01.025.

Logothetis NK. What we can do and what we cannot do with fMRI. Nature 2008;453:869–78. https://doi.org/10.1038/nature06976.

Malenka RC, Bear MF. LTP and LTD: an embarrassment of riches. Neuron 2004;44:5–21. https://doi.org/10.1016/j.neuron.2004.09.012.

Manuel TJ, Kusunose J, Zhan X, Lv X, Kang E, Yang A, et al. Ultrasound neuromodulation depends on pulse repetition frequency and can modulate inhibitory effects of TTX. Sci Rep 2020;10:15347. https://doi.org/10.1038/s41598-020-72189-y.

Marsac L, Chauvet D, La Greca R, Boch A-L, Chaumoitre K, Tanter M, et al. Ex vivo optimisation of a heterogeneous speed of sound model of the human skull for non-invasive transcranial focused ultrasound at 1 MHz. Int J Hyperthermia 2017;33:635–45. https://doi.org/10.1080/02656736.2017.1295322.

McClintock SM, Reti IM, Carpenter LL, McDonald WM, Dubin M, Taylor SF, et al. Consensus Recommendations for the Clinical Application of Repetitive Transcranial Magnetic Stimulation (rTMS) in the Treatment of Depression. J Clin Psychiatry 2018;79:16cs10905. https://doi.org/10.4088/JCP.16cs10905.

McDannold N, Maier SE. Magnetic resonance acoustic radiation force imaging. Med Phys 2008;35:3748–58. https://doi.org/10.1118/1.2956712.

Mehić E, Xu JM, Caler CJ, Coulson NK, Moritz CT, Mourad PD. Increased Anatomical Specificity of Neuromodulation via Modulated Focused Ultrasound. PLOS ONE 2014;9:e86939. https://doi.org/10.1371/journal.pone.0086939.

Meng Y, Hynynen K, Lipsman N. Applications of focused ultrasound in the brain: from thermoablation to drug delivery. Nat Rev Neurol 2021;17:7–22. https://doi.org/10.1038/s41582-020-00418-z.

Meng Y, Jones RM, Davidson B, Huang Y, Pople CB, Surendrakumar S, et al. Technical Principles and Clinical Workflow of Transcranial MR-Guided Focused Ultrasound. Stereotact Funct Neurosurg 2021:1–14. https://doi.org/10.1159/000512111.

Menz MD, Oralkan O, Khuri-Yakub PT, Baccus SA Precise neural stimulation in the retina using focused ultrasound. J Neurosci 2013;33:4550–4560. https://doi.org/10.1523/JNEUROSCI.3521-12.2013.

Menz MD, Ye P, Firouzi K, Nikoozadeh A, Pauly KB, Khuri-Yakub P, et al. Radiation Force as a Physical Mechanism for Ultrasonic Neurostimulation of the Ex Vivo Retina. J Neurosci 2019;39:6251–64. https://doi.org/10.1523/JNEUROSCI.2394-18.2019.

Miller GW, Eames M, Snell J, Aubry JF. Ultrashort echo-time MRI versus CT for skull aberration correction in MR-guided transcranial focused ultrasound: In vitro comparison on human calvaria. Med Phy 2015;42:2223–33. https://doi.org/10.1118/1.4916656.

Min BK, Bystritsky A, Jung KI, Fischer K, Zhang Y, Maeng LS, et al. Focused ultrasound-mediated suppression of chemically-induced acute epileptic EEG activity. BMC Neurosci 2011a;12:23. https://doi.org/10.1186/1471-2202-12-23.

Min BK, Yang PS, Bohlke M, Park S, R.Vago D, Maher TJ, et al. Focused ultrasound modulates the level of cortical neurotransmitters: Potential as a new functional brain mapping technique. International Journal of Imaging Systems and Technology 2011b;21:232–40. https://doi.org/10.1002/ima.20284.

Mohammadjavadi M, Ye PP, Xia A, Brown J, Popelka G, Pauly KB. Elimination of peripheral auditory pathway activation does not affect motor responses from ultrasound neuromodulation. Brain Stimul 2019;12:901–10. https://doi.org/10.1016/j.brs.2019.03.005.

Monti MM, Schnakers C, Korb AS, Bystritsky A, Vespa PM. Non-Invasive Ultrasonic Thalamic Stimulation in Disorders of Consciousness after Severe Brain Injury: A First-in-Man Report. Brain Stimul 2016;9:940–1. https://doi.org/10.1016/j.brs.2016.07.008.

Mueller J, Ai L, Bansal P, Legon W. Numerical evaluation of the skull for human neuromodulation with transcranial focused ultrasound. J Neural Eng 2017;14:066012. https://doi.org/10.1088/1741-2552/aa843e.

Mueller J, Ai L, Bansal P, Legon W. Computational exploration of wave propagation and heating from transcranial focused ultrasound for neuromodulation. J Neural Eng 2016;13:056002. https://doi.org/10.1088/1741-2560/13/5/056002.

Mueller J, Legon W, Opitz A, Sato TF, Tyler WJ. Transcranial Focused Ultrasound Modulates Intrinsic and Evoked EEG Dynamics. Brain Stimul 2014;7:900–8. https://doi.org/10.1016/j.brs.2014.08.008.

Mueller JK. Advancing Transcranial Focused Ultrasound for Noninvasive Neuromodulation of Human Cortex. 2015. https://vtechworks.lib.vt.edu/handle/10919/56578.

Murd C, Luiga I, Kreegipuu K, Bachmann T. Scotomas induced by multiple, spatially invariant TMS pulses have stable size and subjective contrast. Int J Psychophysiol 2010;77:157–65. https://doi.org/10.1016/j.ijpsycho.2010.06.001.

Naor O, Krupa S, Shoham S. Ultrasonic neuromodulation. J Neural Eng 2016;13:031003. https://doi.org/10.1088/1741-2560/13/3/031003.

Navarro de Lara LI, Tik M, Woletz M, Frass-Kriegl R, Moser E, Laistler E, Windischberger C. High-sensitivity TMS/fMRI of the Human Motor Cortex Using a Dedicated Multichannel MR Coil. Neuroimage 2017;150:262-269. https://doi.org/10.1016/j.neuroimage.2017.02.062.

Navarro de Lara LI, Windischberger C, Kuehne A, Woletz M, Sieg J, Bestmann S, Weiskopf N, Strasser B, Moser E, Laistler E. A novel coil array for combined TMS/fMRI experiments at 3 T. Magn Reson 2015;Med 74:1492-1501. https://doi.org/10.1002/mrm.25535.

Nitsche MA, Paulus W: Excitability changes induced in the human motor cortex by weak transcranial direct current stimulation. J Physiol 2000, 527:633–639. https://doi.org/10.1111/j.1469-7793.2000.t01-1-00633.x.

O'Brien WD. Ultrasound-biophysics mechanisms. Prog Biophys Mol Biol 2007;93:212–55. https://doi.org/10.1016/j.pbiomolbio.2006.07.010.

Oh SJ, Lee JM, Kim H-B, Lee J, Han S, Bae JY, et al. Ultrasonic Neuromodulation via Astrocytic TRPA1. Curr Biol 2019;29:3386-3401.e8. https://doi.org/10.1016/j.cub.2019.08.021.

O'Reilly MA, Huang Y, Hynynen K. The impact of standing wave effects on transcranial focused ultrasound disruption of the blood-brain barrier in a rat model. Phys Med Biol 2010;55:5251–67. https://doi.org/10.1088/0031-9155/55/18/001.

Owen SF, Liu MH, Kreitzer AC. Thermal constraints on in vivo optogenetic manipulations. Nat Neurosci 2019;22:1061–5. https://doi.org/10.1038/s41593-019-0422-3.

Ozenne V, Constans C, Bour P, Santin MD, Valabrègue R, Ahnine H, et al. MRI monitoring of temperature and displacement for transcranial focus ultrasound applications. Neuroimage 2020;204:116236. https://doi.org/10.1016/j.neuroimage.2019.116236.

Paquin R, Vignaud A, Marsac L, Younan Y, Lehéricy S, Tanter M, et al. Keyhole acceleration for magnetic resonance acoustic radiation force imaging (MR ARFI). Magn Reson Imaging 2013;31:1695–703. https://doi.org/10.1016/j.mri.2013.07.011.

Pasquinelli C, Hanson LG, Siebner HR, Lee HJ, Thielscher A. Safety of transcranial focused ultrasound stimulation: A systematic review of the state of knowledge from both human and animal studies. Brain Stimul 2019;12:1367–80. https://doi.org/10.1016/j.brs.2019.07.024.

Paus T. Inferring causality in brain images: a perturbation approach. Philos Trans R Soc Lond B Biol Sci 2005;360:1109–14. https://doi.org/10.1098/rstb.2005.1652.

Peng D, Tong W, Collins DJ, Ibbotson MR, Prawer S, Stamp M. Mechanisms and Applications of Neuromodulation Using Surface Acoustic Waves—A Mini-Review. Front Neurosci 2021;15. https://doi.org/10.3389/fnins.2021.629056.

Petersen EN, Chung H-W, Nayebosadri A, Hansen SB. Kinetic disruption of lipid rafts is a mechanosensor for phospholipase D. Nat Commun 2016;7:13873. https://doi.org/10.1038/ncomms13873.

Phipps MA, Jonathan SV, Yang P-F, Chaplin V, Chen LM, Grissom WA, et al. Considerations for ultrasound exposure during transcranial MR acoustic radiation force imaging. Sci Rep 2019;9:16235. https://doi.org/10.1038/s41598-019-52443-8.

Pichardo S, Hynynen K. Treatment of near-skull brain tissue with a focused device using shear-mode conversion: A numerical study. Phys Med and Biol 2008;52:7313–32. https://doi.org/10.1088/0031-9155/52/24/008.

Pichardo S, Sin VW, Hynynen K. Multi-frequency characterization of the speed of sound and attenuation coefficient for longitudinal transmission of freshly excised human skulls. Phys Med Biol 2011;56:219–50. https://doi.org/10.1088/0031-9155/56/1/014.

Pinton G, Aubry JF, Bossy E, Muller M, Pernot M, Tanter M. Attenuation, scattering, and absorption of ultrasound in the skull bone. Med Phys 2012a;39:299–307. https://doi.org/10.1118/1.3668316.

Pinton G, Aubry JF, Fink M, Tanter M. Numerical prediction of frequency dependent 3D maps of mechanical index thresholds in ultrasonic brain therapy. Med Phys 2012b;39:455–67. https://doi.org/10.1118/1.3670376.

Pinton GF, Aubry JF, Tanter M. Direct phase projection and transcranial focusing of ultrasound for brain therapy. IEEE Trans Ultrason Ferroelectr Freq Control 2012;59:1149–59. https://doi.org/10.1109/tuffc.2012.2305.

Pinton GF, Dahl J, Rosenzweig S, Trahey GE. A heterogeneous nonlinear attenuating full-wave model of ultrasound. IEEE Trans Ultrason Ferroelectr Freq Control 2009;56:474–88. https://doi.org/10.1109/TUFFC.2009.1066.

Plaksin M, Kimmel E, Shoham S. Cell-Type-Selective Effects of Intramembrane Cavitation as a Unifying Theoretical Framework for Ultrasonic Neuromodulation. eNeuro 2016;3. https://doi.org/10.1523/ENEURO.0136-15.2016.

Plaksin M, Shoham S and Kimmel E. Intramembrane Cavitation as a Predictive Bio-Piezoelectric Mechanism for Ultrasonic Brain Stimulation. Phys Rev X**4**, 2014;011004. https://doi.org/10.1103/PhysRevX.4.011004.

Pouget P, Frey S, Ahnine H, Attali D, Claron J, Constans C, et al. Neuronavigated Repetitive Transcranial Ultrasound Stimulation Induces Long-Lasting and Reversible Effects on Oculomotor Performance in Non-human Primates. Front Physiol 2020;11. https://doi.org/10.3389/fphys.2020.01042.

Prieto ML, Firouzi K, Khuri-Yakub BT, Madison DV, Maduke M. Spike frequency-dependent inhibition and excitation of neural activity by high-frequency ultrasound. J Gen Physiol 2020;152. https://doi.org/10.1085/jgp.202012672.

Prieto ML, Firouzi K, Khuri-Yakub BT, Maduke M. Activation of Piezo1 but Not NaV1.2 Channels by Ultrasound at 43 MHz. Ultrasound Med Biol 2018;44:1217–32. https://doi.org/10.1016/j.ultrasmedbio.2017.12.020.

Prieto ML, Oralkan Ö, Khuri-Yakub BT, Maduke MC. Dynamic Response of Model Lipid Membranes to Ultrasonic Radiation Force. PLOS ONE 2013;8:e77115. https://doi.org/10.1371/journal.pone.0077115.

Radman T, Ramos RL, Brumberg JC, Bikson M. Role of Cortical Cell Type and Morphology in Sub- and Suprathreshold Uniform Electric Field Stimulation. Brain Stimul 2009;2:215–28. https://doi.org/10.1016/j.brs.2009.03.007.

Ramaswamy K, Marx V, Laser D, Kenny T, Chi T, Bailey M, et al. Targeted microbubbles: a novel application for the treatment of kidney stones. BJU Int 2015;116:9–16. https://doi.org/10.1111/bju.12996.

Rapinesi C, Kotzalidis GD, Ferracuti S, Sani G, Girardi P, Del Casale A. Brain Stimulation in Obsessive-Compulsive Disorder (OCD): A Systematic Review. Curr Neuropharmacol 2019;17:787–807. https://doi.org/10.2174/1570159X17666190409142555.

Reznik SJ, Sanguinetti JL, Tyler WJ, Daft C, Allen JJB. A double-blind pilot study of transcranial ultrasound (TUS) as a five-day intervention: TUS mitigates worry among depressed participants. Neurol Psychiatry Brain Res 2020;37:60–6. https://doi.org/10.1016/j.npbr.2020.06.004.

Rieke V, Butts Pauly K. MR thermometry. J Magn Reson Imaging 2008;27:376–90. https://doi.org/10.1002/jmri.21265.

Riis T, Kubanek J. Effective Ultrasonic Stimulation in Human Peripheral Nervous System. IEEE Trans Biomed Eng 2021:1–1. https://doi.org/10.1109/TBME.2021.3085170.

Rinaldi PC, Jones JP, Reines F, Price LR. Modification by focused ultrasound pulses of electrically evoked responses from an in vitro hippocampal preparation. Brain Res 1991;558:36–42. https://doi.org/10.1016/0006-8993(91)90711-4.

Robertson J, Martin E, Cox B, Treeby BE. Sensitivity of simulated transcranial ultrasound fields to acoustic medium property maps. Phys Med Biol 2017;62:2559–80. https://doi.org/10.1088/1361-6560/aa5e98.

Rohr KR, Rooney JA. Effect of ultrasound on a bilayer lipid membrane. Biophys J 1978;23:33–40. https://doi.org/10.1016/S0006-3495(78)85430-7.

Rossi S, Antal A, Bestmann S, Bikson M, Brewer C, Brockmöller J, et al. Safety and recommendations for TMS use in healthy subjects and patient populations, with updates on training, ethical and regulatory issues: Expert Guidelines. Clin Neurophysiol 2020;132, 269–306. https://doi.org/10.1016/j.clinph.2020.10.003.

Rossini PM, Burke D, Chen R, Cohen LG, Daskalakis Z, Di Iorio R, et al. Non-invasive electrical and magnetic stimulation of the brain, spinal cord, roots and peripheral nerves: Basic principles and procedures for routine clinical and research application. An updated report from an I.F.C.N. Committee. Clin Neurophysiol 2015;126:1071–107. https://doi.org/10.1016/j.clinph.2015.02.001.

Ruohonen J, Karhu J. Navigated transcranial magnetic stimulation. Neurophysiol Clin 2010;40:7–17. https://doi.org/10.1016/j.neucli.2010.01.006.

Ryu S, Pyo D, Lim SC, Kwon DS. Mechanical Vibration Influences the Perception of Electrovibration. Sci Rep 2018;8:4555. https://doi.org/10.1038/s41598-018-22865-x.

Sagi Y, Tavor I, Hofstetter S, Tzur-Moryosef S, Blumenfeld-Katzir T, Assaf Y. Learning in the fast lane: new insights into neuroplasticity. Neuron 2012;73:1195–203. https://doi.org/10.1016/j.neuron.2012.01.025.

Salahshoor H, Shapiro MG, Ortiz M. Transcranial Focused Ultrasound Generates Skull-Conducted Shear Waves: Computational Model and Implications for Neuromodulation. BioRxiv 2020:2020.04.16.045237. https://doi.org/10.1101/2020.04.16.045237.

Sanguinetti JL, Hameroff S, Smith EE, Sato T, Daft CMW, Tyler WJ, et al. Transcranial Focused Ultrasound to the Right Prefrontal Cortex Improves Mood and Alters Functional Connectivity in Humans. Front Hum Neurosci 2020;14. https://doi.org/10.3389/fnhum.2020.00052.

Sarvazyan AP, Rudenko OV, Nyborg WL. Biomedical applications of radiation force of ultrasound: historical roots and physical basis. Ultrasound Med Biol 2010;36:1379–94. https://doi.org/10.1016/j.ultrasmedbio.2010.05.015.

Sarvazyan AP, Rudenko OV, Swanson SD, Fowlkes JB, Emelianov SY. Shear wave elasticity imaging: a new ultrasonic technology of medical diagnostics. Ultrasound Med Biol 1998;24:1419–35. https://doi.org/10.1016/s0301-5629(98)00110-0.

Sato T, Shapiro MG, Tsao DY. Ultrasonic Neuromodulation Causes Widespread Cortical Activation via an Indirect Auditory Mechanism. Neuron 2018;98:1031-1041.e5. https://doi.org/10.1016/j.neuron.2018.05.009.

Schimek N, Burke-Conte Z, Abernethy J, Schimek M, Burke-Conte C, Bobola M, et al. Repeated Application of Transcranial Diagnostic Ultrasound Towards the Visual Cortex Induced Illusory Visual Percepts in Healthy Participants. Front Hum Neurosci 2020;14. https://doi.org/10.3389/fnhum.2020.00066.

Silvanto J, Muggleton NG, Cowey A, Walsh V. Neural adaptation reveals state-dependent effects of transcranial magnetic stimulation. Eur J Neurosci 2007;25:1874–81. https://doi.org/10.1111/j.1460-9568.2007.05440.x.

Silvanto J, Pascual-Leone A. State-Dependency of Transcranial Magnetic Stimulation. Brain Topogr 2008;21:1–10. https://doi.org/10.1007/s10548-008-0067-0.

Sorum B, Rietmeijer RA, Gopakumar K, Adesnik H, Brohawn SG. Ultrasound activates mechanosensitive TRAAK K+ channels through the lipid membrane. PNAS 2021;118. https://doi.org/10.1073/pnas.2006980118.

Stern JM, Spivak NM, Becerra SA, Kuhn TP, Korb AS, Kronemyer D, et al. Safety of focused ultrasound neuromodulation in humans with temporal lobe epilepsy. Brain Stimul 2021;14:1022–31. https://doi.org/10.1016/j.brs.2021.06.003.

Sukovich JR, Cain CA, Pandey AS, Chaudhary N, Camelo-Piragua S, Allen SP, et al. In vivo histotripsy brain treatment. J Neurosurg 2018;131:1331–8. https://doi.org/10.3171/2018.4.JNS172652.

Sun J, Hynynen K. Focusing of therapeutic ultrasound through a human skull: a numerical study. J Acoust Soc Am 1998;104:1705–15. https://doi.org/10.1121/1.424383.

Takagi S, Higashino S, Shibuya T, Osawa N. The Actions of Ultrasound on the Myelinated Nerve, the Spinal Cord and the Brain. Jpn J Physiol 1960;10:183–93. https://doi.org/10.2170/jjphysiol.10.183.

Tan CL, Cooke EK, Leib DE, Lin YC, Daly GE, Zimmerman CA, et al. Warm-Sensitive Neurons that Control Body Temperature. Cell 2016;167:47-59.e15. https://doi.org/10.1016/j.cell.2016.08.028.

Tehovnik EJ, Slocum WM, Schiller PH. Saccadic eye movements evoked by microstimulation of striate cortex. Eur J Neurosci 2003;17:870–8. https://doi.org/10.1046/j.1460-9568.2003.02489.x.

Thielscher A, Kammer T. Electric field properties of two commercial figure-8 coils in TMS: calculation of focality and efficiency. Clin Neurophysiol 2004;115:1697–1708. https://doi.org/10.1016/j.clinph.2004.02.019.

Thielscher A, Opitz A, Windhoff M. Impact of the gyral geometry on the electric field induced by transcranial magnetic stimulation. Neuroimage 2011;54:234–43. https://doi.org/10.1016/j.neuroimage.2010.07.061.

Todd N, Zhang Y, Arcaro M, Becerra L, Borsook D, Livingstone M, et al. Focused ultrasound induced opening of the blood-brain barrier disrupts inter-hemispheric resting state functional connectivity in the rat brain. Neuroimage 2018;178:414–22. https://doi.org/10.1016/j.neuroimage.2018.05.063.

Treeby BE, Jaros J, Rendell AP, Cox BT. Modeling nonlinear ultrasound propagation in heterogeneous media with power law absorption using a k-space pseudospectral method. J Acoust Soc Am 2012;131:4324–36. https://doi.org/10.1121/1.4712021.

Tufail Y, Matyushov A, Baldwin N, Tauchmann ML, Georges J, Yoshihiro A, et al. Transcranial Pulsed Ultrasound Stimulates Intact Brain Circuits. Neuron 2010;66:681–94. https://doi.org/10.1016/j.neuron.2010.05.008.

Tung YS, Marquet F, Teichert T, Ferrera V, Konofagou EE. Feasibility of noninvasive cavitation-guided blood-brain barrier opening using focused ultrasound and microbubbles in nonhuman primates. Appl Phys Lett 2011;98:163704. https://doi.org/10.1063/1.3580763.

Turner JG, Parrish JL, Hughes LF, Toth LA, Caspary DM. Hearing in Laboratory Animals: Strain Differences and Nonauditory Effects of Noise. Comp Med 2005;55:12–23.

Tyler WJ. Noninvasive Neuromodulation with Ultrasound? A Continuum Mechanics Hypothesis. Neuroscientist 2011;17:25–36. https://doi.org/10.1177/1073858409348066.

Tyler WJ, Tufail Y, Finsterwald M, Tauchmann ML, Olson EJ, Majestic C. Remote Excitation of Neuronal Circuits Using Low-Intensity, Low-Frequency Ultrasound. PLOS ONE 2008;3:e3511. https://doi.org/10.1371/journal.pone.0003511.

Udupa K, Tai P, Saha U, Wennberg R, Valiante T, Andrade D, et al. Theta burst transcranial magnetic stimulation to induce seizures in an epilepsy monitoring unit. Brain Stimul 2020;13:1800–2. https://doi.org/10.1016/j.brs.2020.10.009.

Velling, VA, Shklyaruk SP. Modulation of the functional state of the brain with the aid of focused ultrasonic action. Neurosci behav physiol 1988;18: 369-375. https://doi.org/10.1007/BF01193880.

Verhagen L, Gallea C, Folloni D, Constans C, Jensen DE, Ahnine H, et al. Offline impact of transcranial focused ultrasound on cortical activation in primates. ELife 2019;8:e40541. https://doi.org/10.7554/eLife.40541.

Vyas U, Christensen D. Ultrasound Beam Simulations in Inhomogeneous Tissue Geometries Using the Hybrid Angular Spectrum Method. IEEE Trans Ultrason Ferroelectr Freq Control 2012;59:1093–100. https://doi.org/10.1109/TUFFC.2012.2300.

Wang H, Kim M, Normoyle KP, Llano D. Thermal Regulation of the Brain—An Anatomical and Physiological Review for Clinical Neuroscientists. Front Neurosci 2016;9. https://doi.org/10.3389/fnins.2015.00528.

Wang H, Wang B, Normoyle KP, Jackson K, Spitler K, Sharrock MF, et al. Brain temperature and its fundamental properties: a review for clinical neuroscientists. Front Neurosci 2014;8:307. https://doi.org/10.3389/fnins.2014.00307.

Wang Z, Yan J, Wang X, Yuan Y, Li X. Transcranial Ultrasound Stimulation Directly Influences the Cortical Excitability of the Motor Cortex in Parkinsonian Mice. Mov Disord 2020;35:693–8. https://doi.org/10.1002/mds.27952.

Wattiez N, Constans C, Deffieux T, Daye PM, Tanter M, Aubry J-F, et al. Transcranial ultrasonic stimulation modulates single-neuron discharge in macaques performing an antisaccade task. Brain Stimul 2017;10:1024–31. https://doi.org/10.1016/j.brs.2017.07.007.

Webb TD, Leung SA, Rosenberg J, Ghanouni P, Dahl JJ, Pelc NJ, et al. Measurements of the Relationship Between CT Hounsfield Units and Acoustic Velocity and How It Changes With Photon Energy and Reconstruction Method. IEEE Trans Ultrason Ferroelectr Freq Control 2018;65:1111–24. https://doi.org/10.1109/TUFFC.2018.2827899.

Wever EG, Vernon JA, Rahm WE, Strother WF. Cochlear Potentials in the Cat in Response to High-Frequency Sounds. Proc Natl Acad Sci U S A 1958;44:1087–1090. https://doi.org/10.1073/pnas.44.10.1087.

White PJ, Clement GT, Hynynen K. Local frequency dependence in transcranial ultrasound transmission. Phys Med Biol 2006;51:2293–305. https://doi.org/10.1088/0031-9155/51/9/013.

Wu SY, Aurup C, Sanchez CS, Grondin J, Zheng W, Kamimura H, et al. Efficient Blood-Brain Barrier Opening in Primates with Neuronavigation-Guided Ultrasound and Real-Time Acoustic Mapping. Sci Rep 2018;8:7978. https://doi.org/10.1038/s41598-018-25904-9.

Xia X, Fomenko A, Nankoo JF, Zeng K, Wang Y, Zhang J, et al. Time course of the effects of low-intensity transcranial ultrasound on the excitability of ipsilateral and contralateral human primary motor cortex. Neuroimage. 2021;243:118557. https://doi.org/10.1016/j.neuroimage.2021.118557.

Yang PF, Phipps MA, Jonathan S, Newton AT, Byun N, Gore JC, et al. Bidirectional and state-dependent modulation of brain activity by transcranial focused ultrasound in non-human primates. Brain Stimul 2021;14:261–72. https://doi.org/10.1016/j.brs.2021.01.006.

Yang PF, Phipps MA, Newton AT, Chaplin V, Gore JC, Caskey CF, et al. Neuromodulation of sensory networks in monkey brain by focused ultrasound with MRI guidance and detection. Sci Rep 2018;8:7993. https://doi.org/10.1038/s41598-018-26287-7.

Yang PS, Kim H, Lee W, Bohlke M, Park S, Maher TJ, et al. Transcranial focused ultrasound to the thalamus is associated with reduced extracellular GABA levels in rats. Neuropsychobiology 2012;65:153–60. https://doi.org/10.1159/000336001.

Ye PP, Brown JR, Pauly KB. Frequency Dependence of Ultrasound Neurostimulation in the Mouse Brain. Ultrasound Med Biol 2016;42:1512–30. https://doi.org/10.1016/j.ultrasmedbio.2016.02.012.

Yoo S, Mittelstein DR, Hurt RC, Lacroix JJ, Shapiro MG. Focused ultrasound excites neurons via mechanosensitive calcium accumulation and ion channel amplification. BioRxiv 2020:2020.05.19.101196. https://doi.org/10.1101/2020.05.19.101196.

Yoo SS, Bystritsky A, Lee J-H, Zhang Y, Fischer K, Min BK, et al. Focused ultrasound modulates region-specific brain activity. Neuroimage 2011a;56:1267–75. https://doi.org/10.1016/j.neuroimage.2011.02.058.

Yoo SS, Kim H, Min B-K, Eric Franck SP. Transcranial Focused Ultrasound to the Thalamus Alters Anesthesia Time in Rats. Neuroreport 2011b;22:783–7. https://doi.org/10.1097/WNR.0b013e32834b2957.

Yoo SS, Yoon K, Croce P, Cammalleri A, Margolin RW, Lee W. Focused ultrasound brain stimulation to anesthetized rats induces long-term changes in somatosensory evoked potentials. Int J Imaging Syst Technol 2018;28:106–12. https://doi.org/10.1002/ima.22262.

Yoon K, Lee W, Lee JE, Xu L, Croce P, Foley L, et al. Effects of sonication parameters on transcranial focused ultrasound brain stimulation in an ovine model. PLOS ONE 2019;14:e0224311. https://doi.org/10.1371/journal.pone.0224311.

Younan Y, Deffieux T, Larrat B, Fink M, Tanter M, Aubry JF. Influence of the pressure field distribution in transcranial ultrasonic neurostimulation. Med Phys 2013;40:082902. https://doi.org/10.1118/1.4812423.

Yu K, Liu C, Niu X, He B. Transcranial Focused Ultrasound Neuromodulation of Voluntary Movement-related Cortical Activity in Humans. IEEE Trans Biomed Eng 2020:1–1. https://doi.org/10.1109/TBME.2020.3030892.

Yu K, Niu X, Krook-Magnuson E, He B. Intrinsic functional neuron-type selectivity of transcranial focused ultrasound neuromodulation. Nat Commun 2021;12:2519. https://doi.org/10.1038/s41467-021-22743-7.

Zeng K, Darmani G, Fomenko A, Xia X, Tran S, Nankoo J, et al. Induction of human motor cortex plasticity by theta burst transcranial ultrasound stimulation. Ann Neurol (in press)

Zeng X, McGough RJ. Evaluation of the angular spectrum approach for simulations of near-field pressures. J Acoust Soc Am 2008;123:68–76. https://doi.org/10.1121/1.2812579.

Zhang J, Zhou H, Yang J, Jia J, Niu L, Sun Z, et al. Low-intensity pulsed ultrasound ameliorates depression-like behaviors in a rat model of chronic unpredictable stress. CNS Neurosci Ther 2021;27:233–43. https://doi.org/10.1111/cns.13463.

Ziemann U, Siebner HR. Modifying motor learning through gating and homeostatic metaplasticity. Brain Stimul 2008;1:60–6. https://doi.org/10.1016/j.brs.2007.08.003.

Zou J, Meng L, Lin Z, Qiao Y, Tie C, Wang Y, et al. Ultrasound Neuromodulation Inhibits Seizures in Acute Epileptic Monkeys. iScience 2020;23. https://doi.org/10.1016/j.isci.2020.101066.

Figure legends

Figure 1. (A) Low intensity ultrasound is a pressure wave that travels sinusoidally in space. At one point in time (thick maroon curve at t=0), the pressure wave is a sinusoid in space. At one location x_0, with later time points shown as curves of diminishing thickness and color, the pressure wave passes as a function of time as a sinusoid, plotted explicitly in **(B)** as a function of time.

Figure 2. (A) Temporal, **(B)** spatial and **(C)** spatiotemporal characteristics of pulsed ultrasound are shown. Intensity metrics use the spatial and temporal characteristics in the subscripts. While the pulses shown are of only 8 cycles (16 microseconds at f_0=500kHz), typical ultrasound pulses are on the order of milliseconds in duration. Please note that in this figure we reviewed some of the terminology used in ultrasound for imaging purposes (like peak compression and peak rarefaction) and their detailed description is outside of the scope of this manuscript.

Figure 3. Acoustic interactions at the skull. When sound interacts with the skull, it will (1) be reflected (orange arrow), converted to a shear wave (mode conversion, blue arrow), or transmitted (purple arrow). The transmitted wave is refracted and changes direction, potentially resulting in a displaced focus. As the beam propagates through the skull, significant amplitude is lost due to (2) scattering and absorption. The continued beam propagation will ideally form a focus. If the beam transmits to the distal side of the head, it can be reflected again and interact with the incoming wave, forming (3) a standing wave with nodes of higher and lower intensity than the expected focus.

Figure 4. Scale of the ultrasound focus. Focal spot sizes (solid) and steering ranges (dotted line) of commonly used acoustic apertures. **(A)** In humans, hemispherical arrays are capable of generating a milli-meter-scale mostly circular focus that can be steered over multiple centimeters in deep brain regions. The hemisphere covers much of the skull and requires large volumes of coupling fluid. Reduced spherical cap arrays offer similar lateral beam widths and an axial beam length on the order of a centimeter. The reduced amount of coupling fluid required allows spherical caps of this size to be mechanically positioned around the head. The focal length increases with decreasing aperture size and fixed focus single element transducers and arrays consisting of multiple annuli of this size are common. **(B)** Similar sized spherical cap transducers are used in rodents, although the thinner skull allows for higher frequencies (>1 MHz) to be more easily transmitted through the skull. Steerable arrays designed for rodent neuromodulation are uncommon at present but technically feasible. Water-filled acoustic collimators have been frequently used for mouse neuromodulation. Collimators change the focusing of the transducer and should be considered when assessing the ultrasound exposure field.

Figure 5. Proposed mechanisms of transcranial ultrasound stimulation (TUS). **(A)** Acoustic cavitation causes the formation of bubbles inside the neuronal membrane resulting in capacitance

changes or fracture of the cell membrane. **(B)** Lipid rafts sequester intracellular membrane tethered enzymes and limit interactions with membrane bound substrates. **(C)** Increased temperature or **(D)** mechanical force applied to the membrane disrupts lipid rafts resulting in translocation of the enzyme and increasing substrate enzymatic reactions. The emergent molecules alter gating of mechanosensitive ion channels. While ion channels may be both thermo and mechanosensitive, different channels shown in **(C)** and **(D)** emphasize that they may have different sensitivity to temperature or mechanical force.

Figure 1.

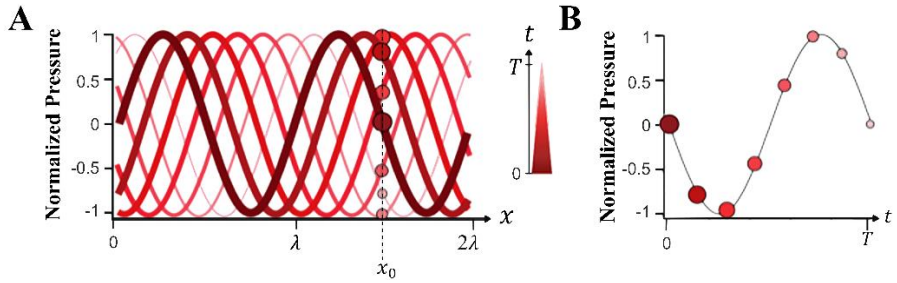

Figure 2.

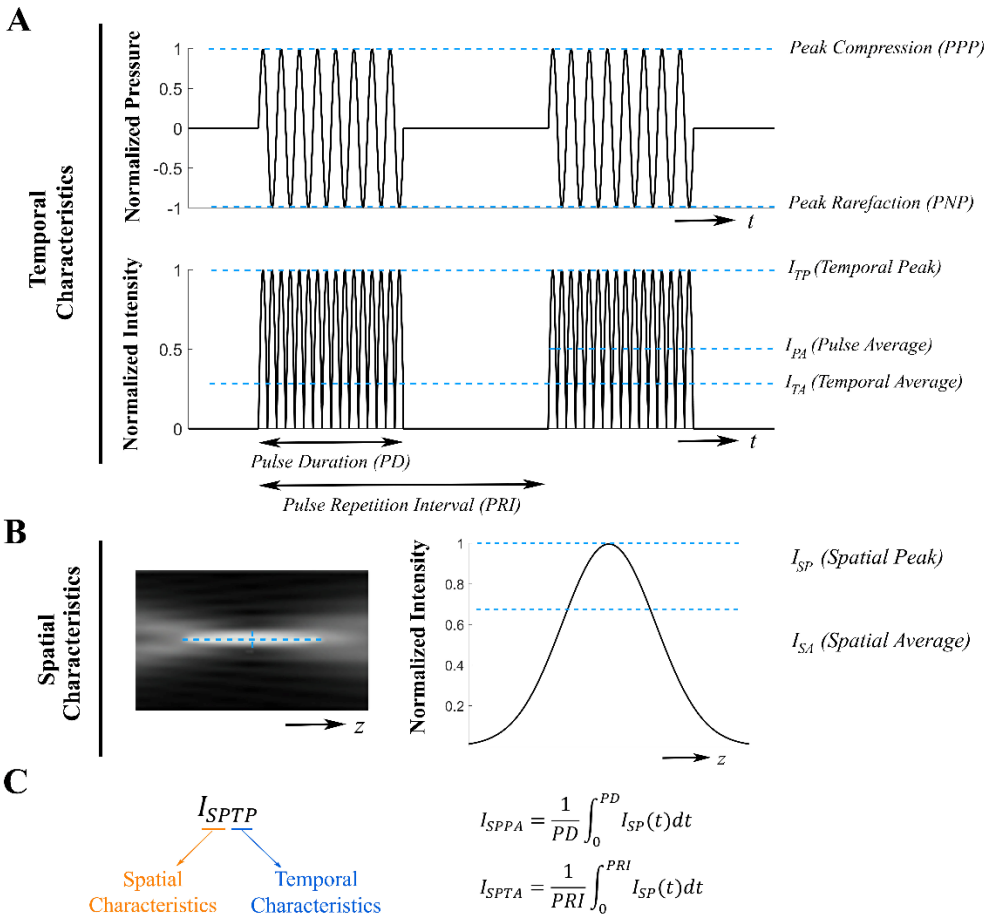

Figure 3.

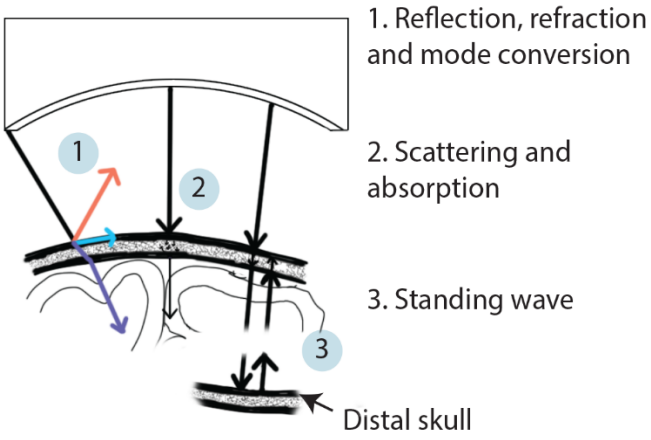

Figure 4.

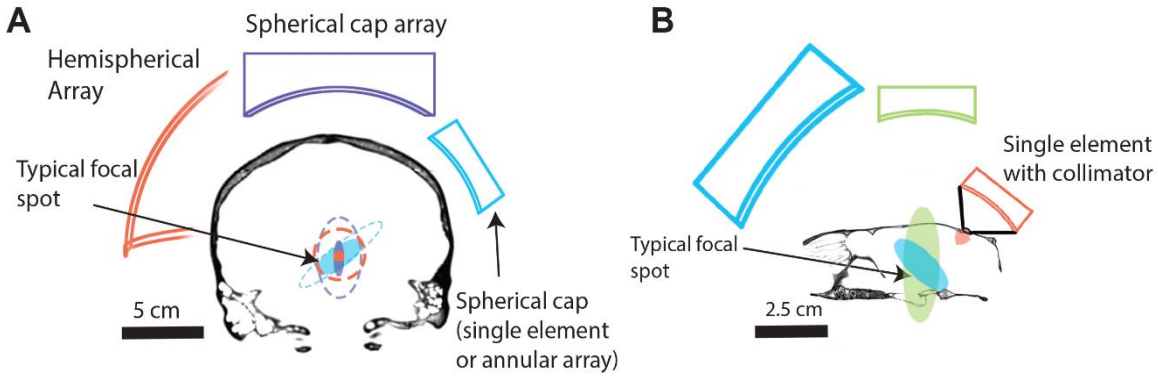

Figure 5.